Heavy δ^{57}Fe in ocean island basalts: a non-unique signature of processes and source lithologies in the mantle

Caroline R. Soderman[a], Simon Matthews[a,1], Oliver Shorttle[a,b], Matthew G. Jackson[c], Saskia Ruttor[d], Oliver Nebel[d], Simon Turner[e], Christoph Beier[f], Marc-Alban Millet[g,2], Elisabeth Widom[h], Munir Humayun[i], Helen M. Williams[g,3]

[a]Department of Earth Sciences, University of Cambridge, Cambridge, CB2 3EQ, UK
[b]Institute of Astronomy, University of Cambridge, Cambridge, CB3 0HA, UK
[c]Department of Earth Science, University of California Santa Barbara, Santa Barbara, CA 93106-9630, USA
[d]School of Earth, Atmosphere and Environment, Monash University, Melbourne, Australia
[e]Department of Earth and Environmental Sciences, Macquarie University, NSW 2109, Australia
[f]Department of Geoscience and Geography, University of Helsinki, FIN-00014 Helsinki, Finland
[g]Department of Earth Sciences, Durham University, Durham, DH1 3LE, UK
[h]Department of Geology & Environmental Earth Science, Miami University, OH 45056, USA
[i]DEOAS & NHMFL, Florida State University, Tallahassee, FL 32310, USA
[1]Present address: Department of Earth and Planetary Sciences, Johns Hopkins University, USA
[2]Present address: School of Earth and Ocean Sciences, Cardiff University, Cardiff, CF10 3AT, UK
[3]Present address: Department of Earth Sciences, University of Cambridge, Cambridge, CB2 3EQ, UK

Abstract

Lithological heterogeneity is a widely accepted feature of the Earth's mantle, with recycled crustal material accounting for a significant part of heterogeneity in ocean island basalt (OIB) geochemistry. Fe isotopes have been used to link geochemical heterogeneity in OIB sources to distinct mantle lithologies due to their mineral-specific equilibrium fractionation effects, or their composition, such as incorporation of kinetically-fractionated core liquids entrained from the core-mantle boundary.

Here we present Fe isotope data for Samoan shield, and Azores volcanoes, together with a combined phase-equilibria and equilibrium mineral-melt isotope fractionation model. These OIB lavas allow us to study the roles of core-derived and recycled mantle components in

generating heavy δ^{57}Fe melts. Heavy δ^{57}Fe correlates with radiogenic isotope signatures of enrichment by a crustal component and not with Fe/Mn or any indicator of core involvement. However, single-stage melting of a MORB-like eclogitic pyroxenite cannot generate the heavy δ^{57}Fe seen in Pitcairn, Azores, and rejuvenated Samoa lavas. Melts of a reaction-zone pyroxenite (commonly suggested to form part of the OIB source), derived from eclogite melts hybridised with peridotite, also fail to generate the heaviest Fe isotopic compositions seen in OIB. Instead, the generation of heavy δ^{57}Fe melts in OIB requires: (1) processes that make subducted eclogite isotopically heavier than its pristine precursor MORB (e.g., hydrothermal alteration, metamorphism, sediment input); (2) lithospheric processing, such as remobilisation of previously frozen small-degree melts, or a contribution from lithospheric material metasomatised by silicate melts; and/or (3) melting conditions that limit the dilution of melts with heavy δ^{57}Fe by ambient lower δ^{57}Fe materials. No single process we consider can generate the heavy δ^{57}Fe seen in the Azores, Pitcairn, and rejuvenated Samoan lavas.

Therefore, it cannot be assumed that a pyroxenite lithology derived from recycled crustal material is the sole producer of heavy δ^{57}Fe melts in OIB, nor can these signatures be related to contributions from the Earth's core. Instead, the observation of heavy δ^{57}Fe OIB melts cannot be ascribed to a unique source or process. This ambiguity reflects the multitude of processes operating from the generation of recycled lithologies through to their mantle melting: from MORB generation, its low temperature alteration, through mantle heterogeneity development and lithospheric processing, to eruption at ocean islands.

1 Introduction

Numerous isotopic and trace element studies of ocean island basalts (OIB) suggest that the Earth's mantle is heterogeneous on scales from hundreds of kilometres, across entire mantle plume systems, to less than a kilometre or metres, as recorded by melt inclusions (e.g., Zindler and Hart, 1986; Weaver, 1991; Hofmann, 1997; Stracke et al., 2005; Maclennan, 2008). The variance in long-lived radiogenic isotopic composition (Sr-Nd-Pb) in most OIB can be explained by mixing between five primary components: depleted mantle, the prevalent mantle (PREMA)/focal zone (FOZO) component, two enriched mantle (EM1/EM2) components and a HIMU component (Stracke, 2012; Fig. 1). Radiogenic isotopes have also been used to argue for enriched (and depleted) components in the mid-ocean ridge basalt source (e.g., Hirschmann and

Stolper, 1996; Salters and Dick, 2002; Liu et al., 2008; Byerly and Lassiter, 2014). In addition to these components, osmium isotopes (Walker et al., 1995; Brandon et al., 1998), combined noble gas and short-lived radiogenic isotopic systematics (e.g., $^{3}He/^{4}He$ and $^{182}W/^{184}W$ anomalies; Mundl et al., 2017; Mundl-Petermeier et al., 2020) and transition element ratios (e.g., Fe/Mn; Humayun et al., 2004) have been used to support the presence of a small amount of a primordial, lower mantle or core-derived component entrained in some OIB.

Linking the heterogeneity in long-lived radiogenic isotopes to mantle lithology has been achieved through combining radiogenic and stable isotopes (e.g., Day et al., 2009, 2010), major element compositions of basalts (Jackson and Dasgupta, 2008; Shorttle and Maclennan, 2011) and trace elements in olivine (e.g., Sobolev et al., 2005, 2007; Herzberg, 2011; Neave et al., 2018). These techniques have led to the widely accepted view that recycled oceanic crust generates a significant amount of the variation seen in OIB geochemistry, along with small contributions from sediments and continental crust (e.g., Cohen and O'Nions, 1982; Hofmann and White, 1982; Weaver, 1991; Chauvel et al., 1992; see also Stracke, 2012). The recycled basaltic component is thought to be present as discrete eclogite or, more commonly, pyroxenite (olivine-poor, pyroxene-rich) lithologies, the latter possibly formed by solid-state or melt reaction of eclogite with ambient peridotite (Sobolev et al., 2007; Herzberg, 2011). However, the success of using major elements to identify pyroxenite in OIB sources may depend on the type of enriched component invoked (Lambart et al., 2013); and due to uncertainties over the melting conditions and role of crustal processes (magma recharge events, mixing, diffusional reequilibration; Matzen et al., 2017; Hole, 2018; Gleeson and Gibson, 2019) it is unclear whether source compositional differences unambiguously control the trace element concentrations in olivine phenocrysts.

Non-traditional stable isotope systems, such as Fe, provide an important, alternative method for identifying lithological heterogeneity (of both enriched and depleted components) in the OIB source. Unlike incompatible trace elements and radiogenic isotopes of incompatible elements, both of which are likely to be disproportionately affected by contributions from enriched mantle components (e.g., Burton et al., 2012), the Fe abundances of melts derived from pyroxenitic and peridotitic source mineralogies are similar (e.g., Sobolev et al., 2005). Therefore, neither pyroxenite nor peridotite lithologies should dominate the Fe isotopic composition of erupted melts, and the Fe isotopic composition of the lavas should reflect the relative contributions

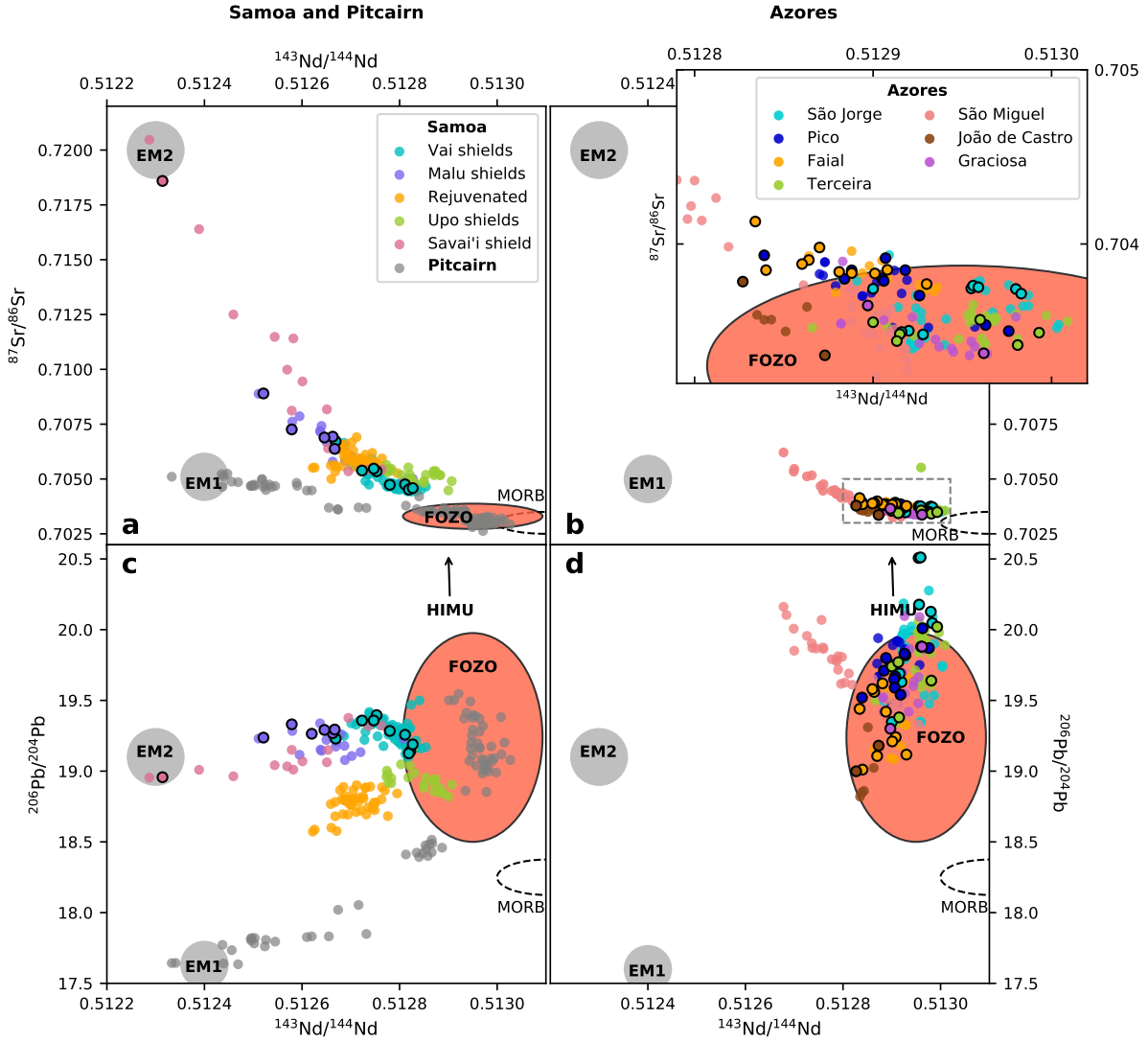

Figure 1: Compilation of Samoa, Pitcairn and Azores radiogenic isotope data showing their different geochemical trends, and comparing them to average MORB (black dashed region; Stracke et al., 2005) and global mantle endmembers (red and grey ovals: EM2 from Jackson et al., 2007b; EM1, HIMU and FOZO – FOZO shown with 2σ uncertainty – from Konter et al., 2008). Samples in this study outlined in black. Pitcairn lavas show a compositional range between FOZO and EM1, Samoan shield lavas between FOZO and EM2 with Samoan rejuvenated lavas showing a weak EM1 component, and Azores lavas between FOZO and HIMU with eastern São Miguel not trending to any global endmember. Samoan data (panels a, c) from Palacz and Saunders (1986); Wright and White (1987); Farley et al. (1992); Hauri and Hart (1993, 1997); Workman et al. (2004); Jackson et al. (2007a,b, 2010, 2014); Hart and Jackson (2014); Pitcairn data (panels a, c) from GEOROC; Azores data (panels b, d) from Turner et al. (1997); Moreira et al. (1999); Beier et al. (2007); Elliott et al. (2007); Beier et al. (2008); Millet et al. (2009); Watanabe (2010); Madureira et al. (2011); Yu (2011); Beier et al. (2012); Hildenbrand et al. (2014); Larrea et al. (2014); Genske et al. (2016); Béguelin et al. (2017); Waters et al. (2020).

from these different lithologies (Williams and Bizimis, 2014). Since Fe isotopes show mineral-specific fractionation effects, they provide a unique opportunity to explore the petrological and mineralogical characteristics of mantle heterogeneity, and could help unravel common melting lithologies and processes in the mantle (Williams and Bizimis, 2014; Konter et al., 2016; Nebel et al., 2018, 2019; Gleeson et al., 2020).

Equilibrium inter-mineral Fe isotope fractionations are driven by the different bonding environments of Fe in mineral structures (Macris et al., 2015; Young et al., 2015). Strong, short Fe–O bonds (due to low coordination numbers and/or the presence of oxidised Fe^{3+}) concentrate heavy Fe, i.e., more ^{57}Fe favoured over ^{54}Fe (Sossi and O'Neill, 2017), which is reported as higher δ^{57}Fe, where

$$\delta^{57}\mathrm{Fe} = \left(\frac{(^{57}\mathrm{Fe}/^{54}\mathrm{Fe})_{\mathrm{sample}}}{(^{57}\mathrm{Fe}/^{54}\mathrm{Fe})_{\mathrm{IRMM-014}}} - 1 \right) \times 1000 \quad (1)$$

This equilibrium fractionation effect suggests that an olivine-dominated peridotite will be isotopically lighter than a more pyroxene-rich (pyroxenite) recycled component (Macris et al., 2015; Sossi and O'Neill, 2017) due to the presence of a small amount of Fe^{3+} in pyroxene, and hence stronger Fe–O bonds, relative to olivine. Similarly, pure iron metal (Fe^0) is expected to be isotopically lighter than lower mantle silicate ($Fe^{2+,3+}$) due to the difference in Fe valence state between the phases (Shahar et al., 2016), although this effect is predicted to be small at pressures and temperatures relevant to core equilibration (Shahar et al., 2016; Liu et al., 2017) and unlikely to be relevant to OIB. Kinetic fractionation effects may also contribute to Fe isotopic variation in OIB melt sources, with thermodiffusion (Soret diffusion) in material diffusing from the outer core into the lowermost mantle recently proposed to generate heavy δ^{57}Fe in entrained plume material (Lesher et al., 2020).

Qualitatively consistent with an isotopically heavy recycled source component, OIB show variable δ^{57}Fe relative to average N- and T-MORB (the latter two dominated by peridotite melting), generally extending to heavier compositions, such as over 0.25‰ in Samoa and Pitcairn. These heavy Fe isotopic compositions are suggested to relate to pyroxenitic mantle components in the OIB source. There are some N-MORB with δ^{57}Fe as heavy as 0.2‰, which could also be consistent with indications of small amounts of enriched pyroxenite or eclogite in the MORB

source (c.f., Hirschmann and Stolper, 1996). The radiogenic isotope systematics of hotspots (plumes) that display heavy δ^{57}Fe signatures show mixing between a common peridotitic mantle component and recycled crustal endmembers (Konter et al., 2016; Nebel et al., 2019; Fig. 1), and in several cases Fe isotopes correlate positively with indices of recycling (e.g., Sr-Nd-Pb isotopes; Nebel et al., 2019). However, it is unclear whether mixing between different mantle components is represented to the same extent in Fe isotopes as in long-lived radiogenic isotopes, and whether Fe and radiogenic isotopic systems can be linked to identify the mineralogy (e.g., pyroxene enrichment) of different mantle components identified in Fig. 1. In using heavy Fe isotopic compositions to better understand mantle heterogeneity, both the sources and processes generating heavy δ^{57}Fe melts in OIB need to be considered.

The Fe isotopic compositions recorded in OIB are heavier (and more variable) than the expected equilibrium isotopic compositions of melts from crustal endmembers contributing to mantle heterogeneity. Isotopic composition estimates for the mantle are $\delta^{57}\text{Fe} = 0.03 \pm 0.03$‰ (DM; Craddock et al., 2013) to 0.05 ± 0.01‰ (BSE; Sossi et al., 2016); for average oceanic crust, represented by MORB, are $\delta^{57}\text{Fe} = 0.15$‰ (Teng et al., 2013; Sossi et al., 2016); and bulk continental crust is indistinguishable from, or lighter than, oceanic crust ($\delta^{57}\text{Fe} = 0.08$–$0.16$‰; Johnson et al., 2020). Highly differentiated ($SiO_2 > 70$ wt%) crust, which could contribute to continentally-derived sediment, records $\delta^{57}\text{Fe} < 0.9$‰ (Du et al., 2017) although the average δ^{57}Fe of rocks with $SiO_2 > 60$ wt% is around 0.3‰ (Johnson et al., 2020). Experimental and theoretical estimates of fractionation during partial mantle melting are known to be small (e.g., Dauphas et al., 2009; Sossi and O'Neill, 2017; Gleeson et al., 2020), likely $\Delta^{57}\text{Fe}_{\text{melt}-\text{mantle}}$ ($= \delta^{57}\text{Fe}_{\text{melt}} - \delta^{57}\text{Fe}_{\text{mantle}}$) < 0.1‰ depending on Fe^{3+} buffering in the mantle (Dauphas et al., 2014). However, data from Pitcairn and Galapagos Spreading Centre lavas require a mantle component with $\delta^{57}\text{Fe} = 0.30$‰ (Nebel et al., 2019; Gleeson et al., 2020). The heaviest isotopic values in OIB from Samoa have previously been explained by combining source heterogeneity, partial melting, and fractional crystallisation effects (Konter et al., 2016). However, even in this multi-process scenario, equilibrium fractionation factors for these processes are required to be high (crystallisation with $\Delta^{57}\text{Fe}_{\text{olivine}-\text{melt}} = -0.45$‰, and mantle melting with $\Delta^{57}\text{Fe}_{\text{melt}-\text{mantle}} > 0.15$‰; Konter et al., 2016), and possibly unrealistically high (Gleeson et al., 2020). It therefore remains unclear if the heaviest Fe isotopic values in OIB ($\delta^{57}\text{Fe} > 0.25$‰) can be explained by simple melting processes of recycled crustal components embedded in ambient

plume mantle.

Samoan rejuvenated lavas (a later, volumetrically less significant stage than the main shield lavas, erupted far from the plume; Natland, 1980) record the heaviest Fe isotopic compositions in the global OIB dataset (Konter et al., 2016). Samoan shield samples also show correlated $^{3}He/^{4}He$-$\mu^{182}W$, with $^{3}He/^{4}He \leq 33.8$ R/R_a (Jackson et al., 2007a) and $\mu^{182}W \geq -17.3$ (Mundl et al., 2017), proposed to relate to core-equilibrated material (Mundl-Petermeier et al., 2020). Thus, Samoan lavas were selected for further Fe isotopic characterisation. We have expanded the shield lava dataset allowing us to study pyroxenite versus core contributions to heavy $\delta^{57}Fe$ liquids, as the two contributions could be associated with other distinct geochemical signatures. The Azores was chosen as a second OIB locality because it shows radiogenic isotopic mixing between a common Azores mantle component and recycled components, so could allow identification of recycled mantle pyroxenite. There may also be a minor lower mantle or core component associated with the Azores plume, identified by raised $^{3}He/^{4}He$ relative to MORB (≤ 18.4 R/R_a; Moreira et al., 2012) and small negative $\mu^{182}W$ anomalies (≥ -9.9; Mundl-Petermeier et al., 2020). Unlike Samoa, the Azores is also (1) a cooler plume ($> 1400°C$; Beier et al., 2012, compared to $> 1600°C$ in Samoa; Putirka et al., 2018) meaning melts of enriched (and possibly heavy $\delta^{57}Fe$) components will be minimally obscured by contemporaneous melting of ambient, relatively depleted mantle; and (2) shows a well spatially-resolved distribution of melts from different components sampled by volcanoes (Béguelin et al., 2017; Beier et al., 2018; Fig. 1). Therefore, Samoa and the Azores offer different perspectives on the links between distinct mantle components and the source of heavy $\delta^{57}Fe$ lavas.

2 Samples and methods

2.1 Samoa

The Samoan islands show an age-progressive volcanic track (Koppers et al., 2011), with a shield building stage influenced by multiple mantle components (Jackson et al., 2014; Fig. 1). These components include the global EM2 endmember, which is distinguished by high $^{87}Sr/^{86}Sr$ relative to FOZO (but FOZO-like $^{206}Pb/^{204}Pb$) and proposed to relate to recycled continental

sediment (White and Hofmann, 1982; Jackson et al., 2007b); and a high $^{3}He/^{4}He$-negative $\mu^{182}W$ common plume component (Jackson et al., 2007a; Mundl et al., 2017), proposed to relate to a contribution from the outer core (Mundl-Petermeier et al., 2020). Recent shield-stage volcanism is split into two sub-parallel and geochemically distinct volcanic chains (Fig. 1), similar to Hawai'i's Loa and Kea trends (Workman et al., 2004; Huang et al., 2011; Koppers et al., 2011): the Vai and Malu trends. Subsequently, rejuvenated lavas have erupted on the older islands of Savai'i and Upolu (Konter and Jackson, 2012). Rejuvenated lavas record heavy Fe isotopic signatures of $\delta^{57}Fe \geq 0.3‰$ (Konter et al., 2016), and an EM1-like component (Workman et al., 2004; Konter and Jackson, 2012; Reinhard et al., 2019; Fig. 1c). Metasomatism of the lithosphere by silicate melts and/or mineralogical heterogeneity (a pyroxenite component) are proposed as the most likely origin of the heavy $\delta^{57}Fe$ in Samoa (Konter et al., 2016).

The 14 new Samoan samples we studied are subaerial and submarine shield lavas, covering six volcanic centres (Savai'i, Tutuila, Malumalu, Ofu, Ta'u and Vailulu'u). These samples cover the range of the long-lived radiogenic isotope space spanned by Samoan shield lavas (Fig. 1), and include high $^{3}He/^{4}He$, negative $\mu^{182}W$ samples (Ofu; Mundl et al., 2017). Major and trace element, and radiogenic isotopic data has been published previously (Vailulu'u and Malumalu seamounts and subaerial Ta'u lavas from Workman et al., 2004; Ofu from Jackson et al., 2007a, 2010; Hart and Jackson, 2014). Only samples with greater than 5 wt% MgO were selected, to limit the effects of fractional crystallisation, particularly magnetite fractionation (Williams et al., 2018). Three high MgO samples (> 18 wt%) were chosen to explore the $\delta^{57}Fe$ variability that could be introduced to lavas by olivine accumulation during melt storage and transport. The Savai'i sample (ALIA115-18) is a dredged lava with heavy $\delta^{57}Fe$ (0.36‰) previously measured by Konter et al. (2016), which was suggested to have undergone seawater alteration based on trace element data (combined high LOI of 4.4 wt% and $Ba/Rb < 6.7$; Konter et al., 2016). This sample was the only sample available where alteration is documented, and therefore was measured to get an idea of the Fe isotopic variability that could be induced by alteration. The other samples do not show a trace element signature of alteration (Fig. S1).

2.2 Azores

The Azores consist of nine volcanic islands, on the west and east of the Mid-Atlantic Ridge, and associated with a triple junction. Many of the islands are still active, with most subaerial lavas less than 1 Myr old (Larrea et al., 2018). The Azores volcanoes sample a number of recycled components identified in radiogenic isotopic space, spanning much of the global variation of OIB (Beier et al., 2018), although the eastern São Miguel component is not a globally-defined endmember (Fig. 1). São Jorge lavas have the most radiogenic $^{206}Pb/^{204}Pb$ from the Azores, a signature attributed to the presence of a HIMU-like recycled oceanic crustal component (Millet et al., 2009). These recycled components are mixed with a common Azores component, but appear to undergo limited mixing with each other (Beier et al., 2018). Limited mixing is hypothesised to occur in part because the Terceira rift drains melts from fusible mantle components to the surface, allowing only short scale horizontal migration and mixing of melts between volcanoes towards the Mid-Atlantic Ridge (Béguelin et al., 2017). However, the presence of a recycled oceanic crustal component in Azores lavas is debated, with uranium series disequilibria (Prytulak and Elliott, 2009) and transition element ratios (Beier et al., 2013) consistent with a garnet peridotite source and not requiring pyroxenite/eclogite. It is also suggested that carbonated peridotitic mantle may be present in the Azores source region (Beier et al., 2013), explaining melting despite a relatively small thermal anomaly (Beier et al., 2012). Additionally, a negative $\mu^{182}W$ signature has been recorded in the Azores, suggesting a lower mantle or core component entrained in the Azores plume (Rizo et al., 2019; Mundl-Petermeier et al., 2020).

Here we present Fe isotope data for São Jorge, Terceira, Pico, Faial, João de Castro and Graciosa. Major and trace element, and radiogenic isotopic data are from Turner et al. (1997); Beier et al. (2008); Millet et al. (2009); Watanabe (2010); Yu (2011); Beier et al. (2010, 2012); Béguelin et al. (2017); Waters et al. (2020). Only samples with MgO $>$ 5 wt% were selected, to limit the effects of fractional crystallisation.

2.3 Methods

Iron isotope analyses were carried out following established procedures (Williams et al., 2005, 2009; Cheng et al., 2014) in the laboratories identified in Table 1. In brief, $\sim$ 20 mg of whole-rock

powders were dissolved in a mixture of HF-HNO_3 on a hotplate at 120°C for up to 72 hours, evaporated to dryness and subsequently refluxed in either 6M HCl (Cambridge/Durham), or concentrated HNO_3 and H_2O_2 (Monash University) to remove fluoride bonds. Samples were taken up in 6M HCl (Cambridge/Durham) or 9M HCl (Monash) for column chemistry. Iron purification was achieved through progressive elution in anion exchange resins (AG1-X4 or AG-MP-1), first of matrix followed by Fe, with purified Fe redissolved in 0.1M HNO_3 for isotopic analysis. Full details of methods are given in the Appendix.

Analyses were performed on a MC-ICP-MS NeptunePlus in Cambridge, Durham and Monash in wet plasma and medium resolution, with sample standard bracketing to the IRMM-014 (or isotopically identical IRMM-524a) standard. The international geological reference materials BHVO-2, BCR-2 and BIR-1 were used to evaluate column chemistry procedures, and give values in agreement with published values (Craddock and Dauphas, 2010; Table S1 in Appendix). The in-house $FeCl_3$ standard was used to assess mass dependence, reproducibility and accuracy in Cambridge and Durham, giving δ^{56}Fe = −0.73 ± 0.03‰ (2 S.D.), δ^{57}Fe = −1.08 ± 0.05‰ in Cambridge and δ^{56}Fe = −0.69 ± 0.03‰, δ^{57}Fe = −1.03 ± 0.05‰ in Durham. The long term 2 S.D. reproducibility of δ^{57}Fe analyses is therefore taken as ± 0.05‰.

3 Results

The measured Fe isotope compositions for Samoa and the Azores are given in Table 1. We discuss the Fe-isotope systematics of the two localities separately below.

3.1 Samoa

The measured Fe isotope composition of Samoan shield lavas ranges from δ^{57}Fe = 0.07–0.21‰ (± 0.02‰, 2 S.E.), with an average of δ^{57}Fe = 0.15‰, coinciding with average MORB (Teng et al., 2013). There is no systematic variation between Vai (δ^{57}Fe = 0.07–0.20‰ ± 0.02‰ 2 S.E.) and Malu (δ^{57}Fe = 0.15–0.21‰ ± 0.02‰ 2 S.E.) trend lavas. Duplicate dissolutions of samples ALIA115-18 and AVON-3-71-22 reproduce within 2 S.D. of each other (Table 1). The shield lava dataset measured in this study is comparable with previously published Samoan

Table 1: Iron isotope data for samples and standards measured in this study. Samples measured at †University of Cambridge, ‡Durham University, §Monash University. *d* represents duplicate dissolution of sample. Data from Konter et al. (2016) for the shared sample with this study is shown for reference, with δ^{57}Fe and 2 S.E. calculated assuming mass dependence from published δ^{56}Fe value. S.E. calculated as S.D./$\sqrt{n}$; n = number of repeat measurements. Major element data sources for Samoa: Workman et al., 2004; Jackson et al., 2007a, 2010; Hart and Jackson, 2014, the Azores: Turner et al., 1997; Beier et al., 2008; Millet et al., 2009; Beier et al., 2010; Yu, 2011; Beier et al., 2012; Waters et al., 2020.

Volcano	Sample	MgO (wt%)	FeO_T (wt%)	δ^{56}Fe (‰)	2 S.D.	2 S.E.	δ^{57}Fe (‰)	2 S.D.	2 S.E.	n
Samoa†										
Savai'i	ALIA115-18	5.09	7.09	0.12	0.05	0.02	0.19	0.05	0.02	7
	ALIA115-18 *d*			0.12	0.04	0.02	0.20	0.01	0.01	3
	Konter, 115-18			*0.24*		*0.04*	*(calc) 0.36*		*0.06*	
Malumalu	AVON-3-77-1	7.62	12.17	0.13	0.03	0.02	0.21	0.05	0.02	4
Malumalu	AVON-3-77-9	8.45	11.08	0.13	0.06	0.03	0.18	0.08	0.03	5
Malumalu	ALIA106-03	6.56	12.97	0.13	0.03	0.01	0.21	0.04	0.01	8
Malumalu	AVON-3-78-1	19.68	11.89	0.10	0.03	0.01	0.15	0.05	0.02	9
Malumalu	AVON-3-76-8	6.27	11.93	0.12	0.04	0.02	0.19	0.07	0.03	5
Tutuila	ALIA112-02	6.68	11.11	0.10	0.04	0.02	0.15	0.04	0.02	6
Ofu	OFU-04-14	16.02	12.70	0.07	0.04	0.01	0.12	0.02	0.01	8
Ofu	OFU-05-18	9.81	12.78	0.07	0.02	0.01	0.12	0.04	0.01	11
Vailulu'u	AVON-3-73-1	7.52	11.26	0.11	0.01	0.01	0.14	0.03	0.01	5
Vailulu'u	AVON-3-70-9	6.47	11.65	0.10	0.04	0.02	0.16	0.05	0.02	6
Vailulu'u	AVON-3-63-2	23.87	10.39	0.08	0.03	0.01	0.13	0.04	0.02	5
Vailulu'u	AVON-3-71-22	21.79	10.77	0.05	0.06	0.02	0.07	0.07	0.02	11
	AVON-3-71-22 *d*			0.08	0.01	0.01	0.13	0.04	0.02	3
Ta'u	T33	12.40	11.61	0.12	0.03	0.01	0.21	0.03	0.02	4
Azores										
São Jorge	SJ01‡	8.24	10.43	0.20	0.02	0.01	0.34	0.05	0.02	5
São Jorge	SJ05‡	8.95	12.05	0.13	0.06	0.03	0.24	0.05	0.03	4
São Jorge	SJ07‡	8.45	11.56	0.14	0.02	0.01	0.24	0.08	0.03	6
São Jorge	SJ50‡	8.84	10.70	0.14	0.04	0.02	0.22	0.06	0.03	3
São Jorge	SJ51‡	11.99	11.18	0.18	0.04	0.02	0.23	0.03	0.02	5
São Jorge	SJ52‡	8.20	11.59	0.14	0.02	0.01	0.23	0.03	0.01	6
São Jorge	SJ30 ‡	9.70	11.32	0.17	0.05	0.03	0.28	0.07	0.04	3
São Jorge	SJ31b‡	8.91	12.40	0.25	0.09	0.05	0.28	0.04	0.02	3
São Jorge	WASJ18‡	9.72	10.35	0.20	0.06	0.02	0.28	0.06	0.02	6
Terceira	T2‡	5.54	10.53	0.12	0.03	0.02	0.14	0.03	0.02	3
Terceira	T6‡	8.70	11.03	0.14	0.05	0.03	0.16	0.04	0.02	3
Terceira	T18‡	7.94	10.48	0.16	0.04	0.02	0.22	0.02	0.01	5
Terceira	WAT3‡	11.80	8.68	0.15	0.02	0.01	0.20	0.02	0.01	4
Terceira	AZT-03-12§	5.45	12.44	0.02	0.00	0.00	0.05	0.03	0.02	3
Terceira	AZT-03-016§	5.67	10.88	0.07	0.04	0.02	0.13	0.03	0.02	3
Pico	P4‡	10.36	9.94	0.14	0.04	0.03	0.18	0.03	0.02	2
Pico	P5‡	9.63	9.80	0.20	0.06	0.04	0.24	0.02	0.02	2
Pico	P25‡	8.24	9.99	0.18	0.05	0.02	0.22	0.05	0.02	5
Pico	P26‡	10.83	10.28	0.16	0.03	0.01	0.24	0.05	0.02	6
Pico	P29‡	8.16	9.31	0.22	0.08	0.04	0.28	0.05	0.02	4
Pico	WAP9‡	13.21	9.14	0.15	0.03	0.02	0.17	0.06	0.04	2
Pico	AZP-03-10§	6.60	10.82	0.16	0.03	0.02	0.24	0.03	0.02	3
Pico	AZP-03-23§	5.79	11.41	0.17	0.04	0.02	0.25	0.05	0.03	3
Pico	AZP-03-50§	6.00	10.53	0.17	0.02	0.01	0.27	0.00	0.00	3
Faial	F/FG-28‡	8.13	9.75	0.18	0.06	0.03	0.26	0.03	0.01	5
Faial	F/CP-18‡	7.83	9.32	0.20	0.03	0.01	0.27	0.02	0.01	6
Faial	F/CA-6‡	9.73	9.66	0.20	0.03	0.01	0.26	0.04	0.02	5
Faial	F/CA-24‡	13.99	10.21	0.15	0.07	0.04	0.19	0.03	0.02	4
Faial	WAF1a‡	13.51	9.77	0.14	0.08	0.04	0.26	0.05	0.03	4
Faial	AZF-03-11§	5.47	9.73	0.23	0.01	0.01	0.34	0.03	0.02	3
João de Castro	525DS2§	15.78	10.74	0.14	0.02	0.01	0.27	0.00	0.00	3
João de Castro	523DS2§	6.25	9.34	0.15	0.01	0.01	0.21	0.05	0.03	2
Graciosa	AZG-03-07§	8.17	10.36	0.26	0.04	0.02	0.37	0.02	0.01	2
Graciosa	AZG-03-28§	7.02	9.52	0.18	0.02	0.01	0.27	0.08	0.04	3

shield data (Konter et al., 2016). The rejuvenated lavas from Konter et al. (2016) are much heavier (δ^{57}Fe > 0.3‰) than any of the combined dataset of shield lavas. Our measurement of sample ALIA115-18, the common sample between the two studies, is Δ^{57}Fe = 0.18‰ lighter than that reported by Konter et al. (2016).

3.2 Azores

The Fe isotope composition of Azores samples shows considerable variation, ranging from δ^{57}Fe = 0.05–0.37‰ (± 0.02‰ 2 S.E.), with all but three samples displaying δ^{57}Fe > 0.15‰ (average MORB, Teng et al., 2013) even at the same MgO content as MORB (Fig. 2). Two of these are Terceira samples (T2, AZT-03-016) with slightly low TiO_2 for their MgO (Fig. S4), which may indicate they have experienced early magnetite saturation (Williams et al., 2018) or formed as a result of mixing between primitive melts unsaturated in magnetite and magnetite-saturated evolved melts, and therefore are not considered further. No samples have Ba/Rb < 9, and there is no correlation between δ^{57}Fe and Ba/Rb or LOI (Fig. S2). There is no apparent difference in δ^{57}Fe between different islands.

4 What processes could generate heavy δ^{57}Fe liquids?

Several processes can modify the whole rock δ^{57}Fe from the primary liquid δ^{57}Fe, and the primary liquid δ^{57}Fe from the isotopic composition of ambient peridotite (0.05‰). In this section, we consider how: (1) post melt emplacement processing (fractional crystallisation, olivine accumulation); (2) partial melting; and (3) pre-melt emplacement considerations of mantle lithological heterogeneity, may contribute to the heavy δ^{57}Fe ($\gtrsim$ 0.20‰) seen in Samoa and the Azores.

4.1 Olivine accumulation and fractional crystallisation

Olivine accumulation is known to produce light whole-rock δ^{57}Fe (Teng et al., 2008; McCoy-West et al., 2018). Olivine accumulation is likely for three Samoan samples measured here, as they have high (> 18 wt%) MgO content (Fig. 2). It is possible to correct for olivine accumualation by modelling the removal of olivine (e.g., McCoy-West et al., 2018), however it is unlikely that

the melt has accumulated olivine that is in equilibrium with the final bulk composition which makes the correction hard to use with reliability. Since there is no statistical δ^{57}Fe difference between the high and low MgO shield lavas, we include the (uncorrected) high MgO samples in following plots.

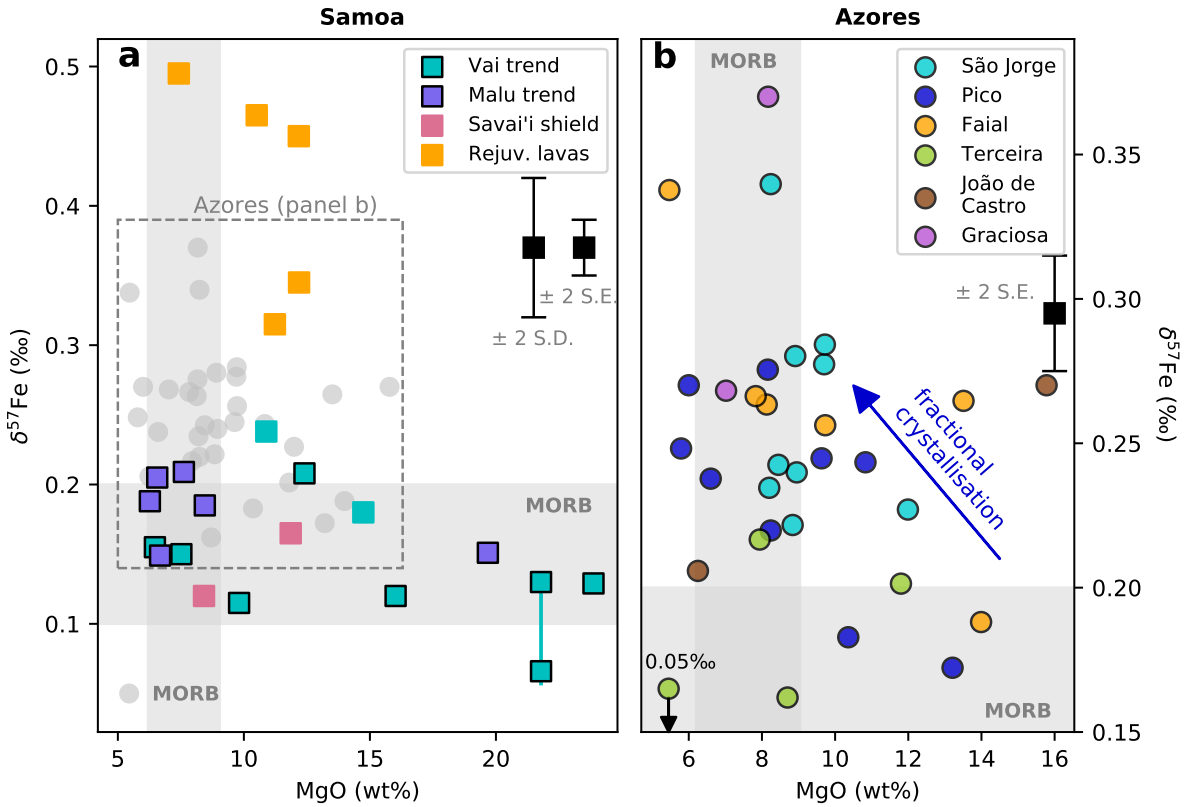

Figure 2: Measured Fe isotope data vs whole-rock MgO: black outlines, data from this study; no outline, data from Konter et al. (2016). At the same MgO content as MORB, the Azores lavas and Samoan rejuvenated lavas are relatively isotopically heavy. Samoan samples with MgO > 18 wt% that have accumulated olivine show no resolvable Fe isotopic difference from lower MgO samples. Some Azores volcanoes (Pico, Faial) show evidence for fractional crystallisation trends. Shaded region is average MORB (δ^{57}Fe from Teng et al., 2013; MgO from range of 'ALL MORB' from Gale et al., 2013). Errorbars show average long term 2 S.D. and average 2 S.E. on repeat measurements; duplicate dissolutions of the same sample linked by a vertical line.

The removal of light δ^{57}Fe mineral phases (e.g., olivine and pyroxene, both isotopically light relative to melt) by fractional crystallisation is an important control on driving the δ^{57}Fe of residual melts to heavier values (e.g., Teng et al., 2008). This isotopic fractionation is thought to be caused by the low Fe^{3+} content of olivine and pyroxene (Dauphas et al., 2014) and is consistent with the MgO–δ^{57}Fe trend seen in Pico lavas (Fig. 2b). Previous studies have shown that fractional crystallisation corrections can be large (Δ^{57}Fe up to −0.15‰ for Pitcairn samples; Nebel et al., 2019, with the biggest corrections for the lowest wt% MgO samples), therefore we perform the same correction to samples with < 18 wt% MgO in this dataset. For

each sample, we incrementally add equilibrium olivine back into our melt composition until the liquid is in equilibrium with Fo_{90} olivine. Given the MgO range of Samoa and Azores samples, pyroxene likely crystallised from these melts (e.g., Beier et al., 2012). However, pyroxene–melt fractionation is expected to be smaller than olivine–melt fractionation (Macris et al., 2015) due to the differing Fe bonding environment in olivine and pyroxene, although the fractionation is poorly constrained. Therefore, we only correct for olivine crystallisation, which provides an upper limit on the fractional crystallisation correction.

The olivine–melt fractionation factor ($\Delta^{57}Fe_{ol-melt}$) generates significant uncertainty in the fractional crystallisation correction used by Sossi et al. (2016) and Nebel et al. (2019). Fig. 3 shows how the magnitude of the correction varies with $\Delta^{57}Fe_{ol-melt} = -0.1\times\ 10^6/T^2$ (calculated using force constants following Sossi and O'Neill, 2017; see Appendix) to $\Delta^{57}Fe_{ol-melt} = -0.4 \times 10^6/T^2$ (following Nebel et al., 2019). Since we are interested in the heavy Fe isotope signatures, we use the largest fractional crystallisation correction, even though this may be overcorrecting the data. The correction therefore represents an upper limit on $\Delta^{57}Fe$ during fractional crystallisation, which will be conservative from the perspective of diminishing as much heavy $\delta^{57}Fe$ enrichment that is observed as possible.

This calculation has been applied to all the MORB and OIB data shown in Fig. 4a. After accounting for the processes of olivine accumulation and fractional crystallisation, the Samoan and Azores datasets still show heavy Fe isotopic compositions relative to MORB (Figs. 3, 4), which must then be a mantle source-derived signal.

4.2 Heterogeneity derived from the mantle

Variability in the Fe isotopic composition of primary mantle melts could be the result of partial melting and/or heterogeneous mantle domains. Mantle heterogeneity is well-studied in the Samoa, Pitcairn and Azores plumes, with different mantle components well-characterised in radiogenic isotope space (Eisele et al., 2002; Jackson et al., 2014; Beier et al., 2018; Waters et al., 2020; Fig. 1). Differences in mantle mineralogy associated with these components may account for variations in Fe isotope composition (Williams and Bizimis, 2014; Konter et al., 2016), as suggested for Pitcairn, where a negative Fe-Pb correlation is interpreted as mixing

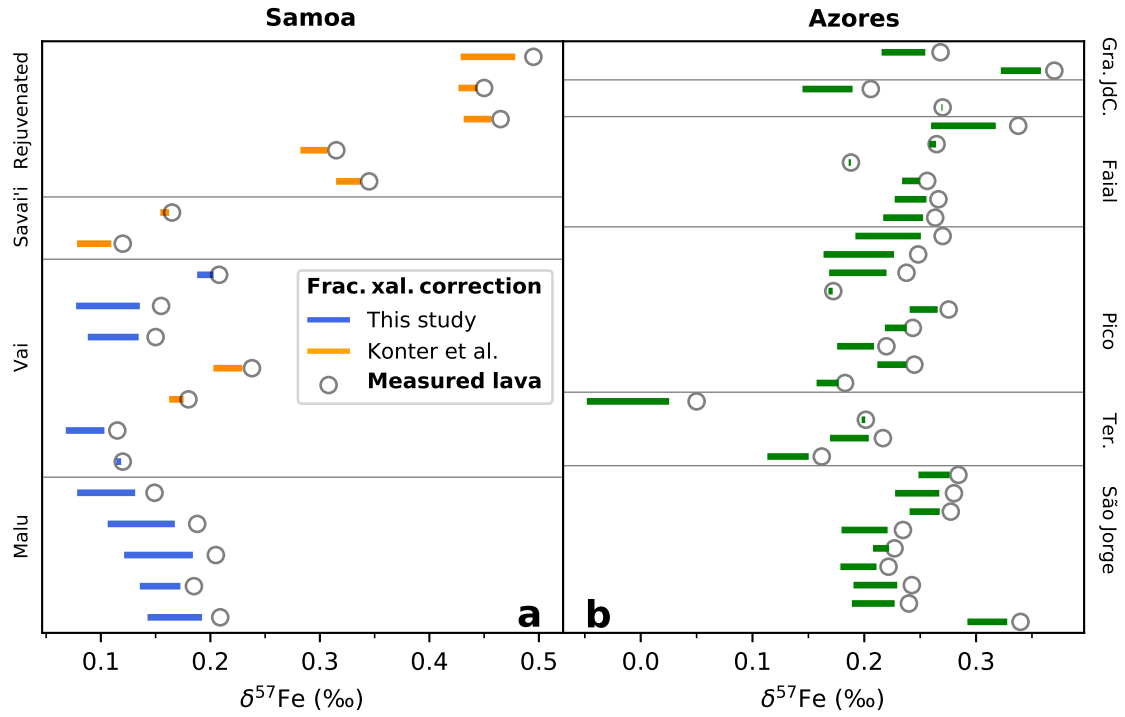

Figure 3: Fractional crystallisation correction following Nebel et al. (2019) and Sossi et al. (2016). The coloured bars show the magnitude of the correction for values of $\Delta^{57}Fe_{ol-melt} = -0.1 \times 10^6/T^2 - -0.4 \times 10^6/T^2$. Using the smaller correction gives corrected values that are unresolvable from the internal precision of the data collected in this study. Uncorrected data shown in outline for comparison. Samples with MgO > 18 wt% were not corrected and are not shown. Abbreviations: 'Gra.': Graciosa; 'JdC.': João de Castro; 'Ter.': Terceira.

between a FOZO-like peridotite and an EM1, heavy δ^{57}Fe pyroxenite (Nebel et al., 2019; Fig. 5). In Samoa, the distinct populations of shield and rejuvenated lavas also form a negative δ^{57}Fe-^{206}Pb/^{204}Pb array (Fig. 5); the heavy δ^{57}Fe endmember is associated with the less radiogenic Pb component. Although the Azores data as a whole shows no Fe-Pb correlation, despite Pb isotopic variability, the island of São Jorge does display a statistically significant correlation distinguishable with external 2 S.D. precision on each sample. However, while we note that the São Jorge samples with the more radiogenic Pb isotopic signature do not show the heaviest δ^{57}Fe (Fig. 5), the spread of δ^{57}Fe in São Jorge is small, so a link between the Pb isotopes and high δ^{57}Fe may be largely masked by analytical precision in this case.

All three plumes produce melts that have heavier δ^{57}Fe than MORB, and show Pb isotopic variability reflecting different components in the mantle source. The likely dominant endmember lithologies responsible for mantle heterogeneity are peridotite (anhydrous or volatile-rich) and pyroxenite derived from recycled oceanic crust (Section 1). Therefore, we first examine whether melting of these endmember lithologies can generate the heavy δ^{57}Fe seen in Samoa, Pitcairn

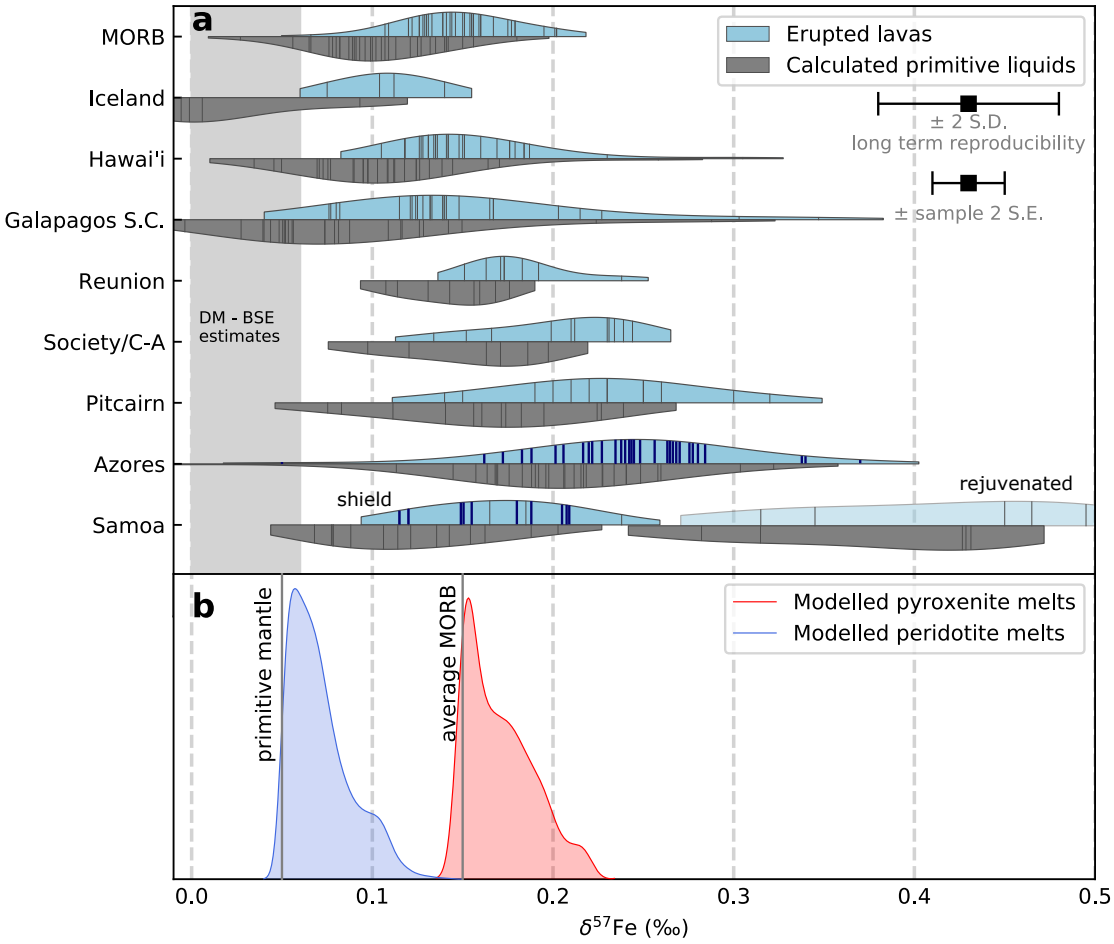

Figure 4: **a**) Compilation of kernel density plots of OIB and MORB Fe isotope data, with each vertical line a sample (bold lines are samples measured in this study). OIB data filtered to only include samples with 5–16 wt% MgO; top errorbar shows long term reproducibility 2 S.D. on δ^{57}Fe of standards run at the University of Cambridge. Samoan rejuvenated lavas record the heaviest δ^{57}Fe in the global dataset, whereas the Samoan shield dataset is indistinguishable from MORB. The Azores show the isotopically heaviest lavas after Samoan rejuvenated lavas. Only normal (N-MORB) and transitional (T-MORB) class MORB data is shown, following the classification by Teng et al., 2013. Data sources: MORB, Teng et al. (2013); Pitcairn, Nebel et al. (2019); Iceland, Schuessler et al. (2009); La Réunion, Peters et al. (2019); Society and Cook-Austral, Teng et al. (2013); Galapagos Spreading Centre, Gleeson et al. (2020); Hawai'i, Teng et al. (2008, 2013); Samoa, Konter et al. (2016), this study; Azores, this study. Fractional crystallisation correction shows liquids calculated to be in equilibrium with Fo_{90} olivine, described in section 4.1. Shaded region shows range of estimates, including quoted errors, for depleted mantle, DM (Craddock et al., 2013; Johnson et al., 2020) and Bulk Silicate Earth, BSE (Sossi et al., 2016). **b**) Model results of compositions of melts of a peridotite (KLB1) and pyroxenite (G2) lithology, discussed in section 4.2.1. Primitive mantle estimate of δ^{57}Fe = 0.05‰ (Sossi et al., 2016) is shown.

and the Azores.

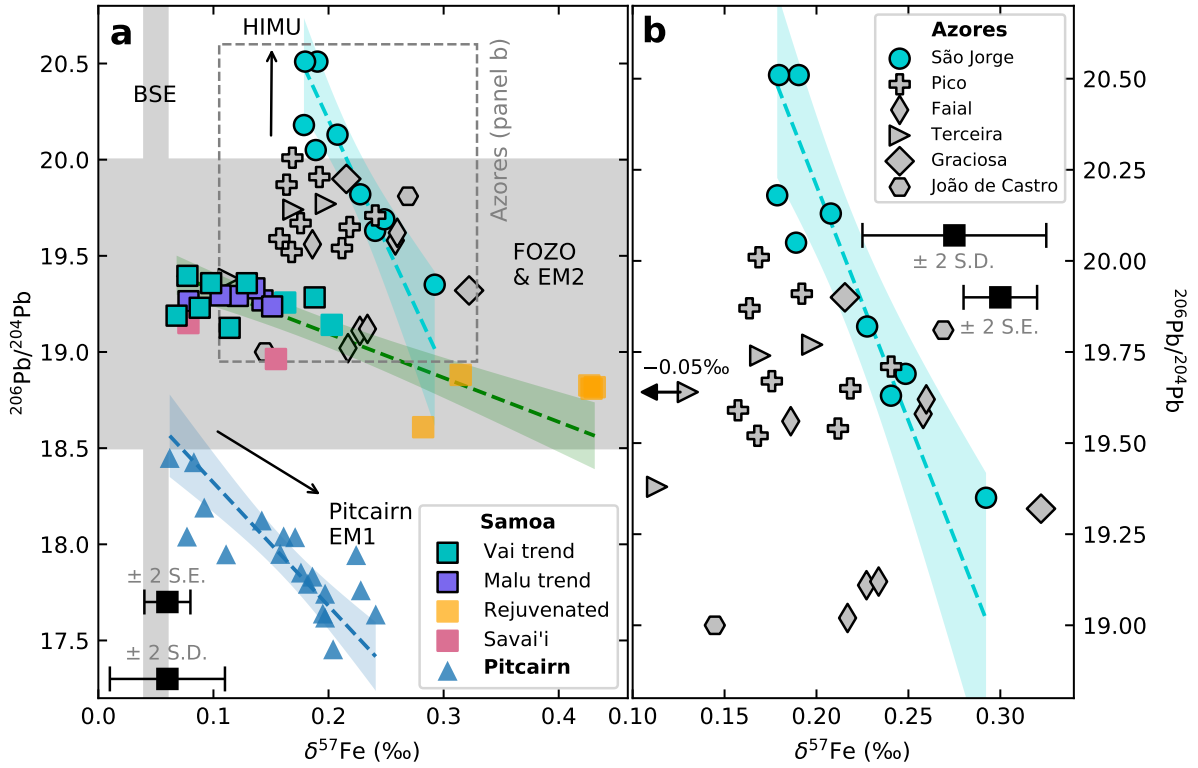

Figure 5: Lead and Fe isotopic variability in the Samoan, Azores and Pitcairn plumes. Data shown have been corrected for fractional crystallisation (Section 4.1). Black outlines indicate iron isotope measurement in this study; no outline indicates published iron isotope data (Samoa, Konter et al., 2016; Pitcairn, Nebel et al., 2019). The plumes show negative arrays with heavy δ^{57}Fe components also having less radiogenic Pb isotopic compositions within each array: orthogonal distance regression lines and 2σ confidence bands for Pitcairn, Samoa, and São Jorge are shown, calculated by weighting each data point with the sample 2 S.D. if known, or the long term 2 S.D. whichever is greater, as errors on δ^{57}Fe.

4.2.1 Iron isotope fractionation by peridotite melting

First, we consider the contribution of anhydrous peridotite melting to the generation of heavy Fe isotopic signatures in OIB. To estimate the heaviest Fe isotopic composition of melts generated from single-stage melting of mantle peridotite, we calculated the modal mineralogy of KLB1 peridotite (a commonly used experimental composition used as an analogue for the upper mantle, based on a Kilborne Hole spinel lherzolite xenolith; see Davis et al., 2009 and Table S2) over P-T space (5–40 kbar, 1100–1930°C) using the dataset of Holland et al. (2018), implemented in THERMOCALC (Powell et al., 1998). Taking the calculated modal mineralogies, the Fe isotope compositions of the phases present (including melts) were calculated using force constants (see Appendix) following Sossi and O'Neill (2017).

The KLB1 pseudosection, showing equilibrium phase assemblages, and melt δ^{57}Fe fractionation results (reported as $\Delta^{57}\text{Fe} = \delta^{57}\text{Fe}_{\text{melt}} - \delta^{57}\text{Fe}_{\text{bulk}}$) are shown in Fig. 6a & c. The maximum partial melting fractionation is small (Δ^{57}Fe = 0.07‰), consistent with estimates from previous studies of Δ^{57}Fe (0.07–0.11‰; Dauphas et al., 2009; Williams and Bizimis, 2014; Sossi et al., 2016; Gleeson et al., 2020). Superimposing this melting fractionation onto the bulk BSE δ^{57}Fe (0.05‰; Sossi et al., 2016) generates insufficiently heavy melts to explain many of the fractional-crystallisation-corrected OIB data. Some MORB also show heavier δ^{57}Fe than would be expected for melting of homogeneous peridotite.

Role of carbonated peridotite melting: Small-degree (carbonatite) melts from a carbonated peridotite mantle have been proposed to explain geochemical variability in Azores lavas (Beier et al., 2013), and carbonatite metasomatism has been proposed to explain trace element data in peridotite xenoliths from Savai'i (Hauri et al., 1993). It is important to consider the role of carbonatite melts in generating heavy δ^{57}Fe lavas because, although carbonatites in equilibrium with silicate mantle are predicted to have $\delta^{57}\text{Fe} < -0.45$‰, some measured intrusive carbonatites extend up to δ^{57}Fe = 1.2‰ (Johnson et al., 2010). Some of these heavy isotopic compositions are attributed to the addition of a heavy δ^{57}Fe (Fe^{3+} rich) fluid at the edges of a carbonatite intrusion in the upper crust (generating compositions of $\delta^{57}\text{Fe} \lesssim 0.6$‰), and other disequilibrium processes including phenocryst mixing, although the complete process of generation of the measured heavy δ^{57}Fe in carbonatites relevant to OIB lavas is unclear.

Carbonated peridotite melts can be identified by their fractionation of trace and major element ratios, including Nb/La, Ti/Sm and K/La (Cottrell and Kelley, 2013; Beier et al., 2013) relative to anhydrous peridotite melts. However, the Azores samples in this study show no relationship between δ^{57}Fe and these ratios (Figs. S6, S7). Beier et al. (2013) suggest that the low Ti/Sm and K/La signature of carbonatite will be obscured by the contribution from peridotitic melts if the contribution of carbonatite in the final melt is $< 20\%$, or the anhydrous ambient peridotite undergoes $> 4\%$ partial melting. By mass balance, with (1) 20% carbonatite; (2) equal proportions of Fe in carbonated peridotite melts and anhydrous peridotite melts (Dasgupta et al., 2009); and (3) volatile-free peridotite δ^{57}Fe = 0.05‰ (Sossi et al., 2016), producing an average fractional-crystallisation-corrected δ^{57}Fe for Azores lavas of 0.20‰ requires $\delta^{57}\text{Fe}_{\text{carbonatite}}$ = 0.8‰. If the carbonatite contribution is 10%, the required $\delta^{57}\text{Fe}_{\text{carbonatite}}$ = 1.55‰. While

the lightest of these hypothetical carbonatite compositions are consistent with some measured intrusive carbonatites, in general carbonatite lavas show significantly lighter δ^{57}Fe compositions (Johnson et al., 2010). Therefore, it seems unlikely that carbonatite melts are contributing to the heavy δ^{57}Fe in Azores lavas, despite the possible presence of a carbonated peridotite lithology in their source region (Beier et al., 2013).

4.2.2 Iron isotope fractionation by pyroxenite melting

Given that pure peridotite melts cannot account for heavy δ^{57}Fe in Samoa, Pitcairn and the Azores, we now consider the effect of using a pyroxenite lithology on Δ^{57}Fe during partial melting. We follow Lambart et al. (2016) in using the term pyroxenite to refer to pyroxene-rich rocks with insufficient olivine ($< 40\%$) to be considered peridotites (Le Maitre et al., 2005). There are a number of recorded natural pyroxenite compositions, but it is unclear which pyroxenite types may best explain global Fe isotopic variability. Natural pyroxenites can be broadly separated into two types: silica-deficient (SD) and silica-excess (SE); producing distinct partial melt compositions (Kogiso et al., 2004; Lambart et al., 2016). Most previously studied pyroxenites are SD type; those that are MgO-rich are thought to be cumulates produced by the fractional crystallisation of peridotite partial melts (Gonzaga et al., 2010; Lambart et al., 2016). Following Lambart et al. (2016), eclogites (from recycled oceanic crust or sediment) and pyroxenites produced from hybridisation between silica-rich eclogite melts and peridotite (Sobolev et al., 2005) are SE type. Previous studies have proposed that the pyroxenitic component in the OIB mantle source may be formed by this hybridisation process (e.g., Sobolev et al., 2005, 2007; Nebel et al., 2019), therefore we consider the melting of SE eclogitic pyroxenite first. Lithospheric pyroxenites with a cumulate origin, possibly through multi-stage processes, are discussed in Section 5.4.

The G2 composition (Table S2), an important MORB-like bulk composition in melting experiments and models from Pertermann and Hirschmann (2003*a*,*b*) and Lambart et al. (2016), is a low MgO quartz eclogite and a SE pyroxenite endmember (Lambart et al., 2016). This eclogitic pyroxenite composition should have a heavier bulk δ^{57}Fe composition than peridotite, at least as heavy as mean MORB (Section 4.2.3). The G2 equilibrium phase assemblage was modelled in the same way as for KLB1 (Fig. 6b) to give the partial melting δ^{57}Fe fractionation over P-T

space (Fig. 6d).

The maximum calculated partial melting fractionation for G2 is small (Δ^{57}Fe = 0.07‰) and similar compared to that of KLB1, although the P-T distribution of melt compositions is different owing to the different melting behaviours of the two lithologies. Iron isotope fractionation during partial melting of individual endmember lithologies alone cannot explain the range in δ^{57}Fe observed for OIB. Therefore, we consider the role of bulk δ^{57}Fe enriched mantle compositions in producing the observed δ^{57}Fe of melts from a two lithology mantle.

4.2.3 Effect of bulk δ^{57}Fe compositions of peridotite and pyroxenite

The pyroxenite bulk δ^{57}Fe is not expected to be the same as that of peridotite (e.g., Williams and Bizimis, 2014; Konter et al., 2016). For eclogitic G2 pyroxenite, which was chosen to be similar in major element chemistry to average modern oceanic crust (Pertermann and Hirschmann, 2003*b*), our initial assumption of starting Fe isotopic composition is that of average MORB (δ^{57}Fe = 0.15‰; Teng et al., 2013; Williams and Bizimis, 2014), although the effect of subduction and eclogite formation during high P, low T metamorphism is poorly understood (Section 5.2.1).

The model results (Fig. 4) show that, based on this assumed G2 starting composition and single-stage melting of each lithology, mixed peridotite and eclogitic pyroxenite melts span the Fe isotope range of Samoan shield and some Azores melts. However, the heaviest of the Samoan and Azores melts (δ^{57}Fe > 0.2‰) require that they are almost pure pyroxenite melts. Although melts derived from a dominantly or exclusively pyroxenitic source have been proposed for Hawai'i based on olivine compositions (Sobolev et al., 2005; Herzberg, 2011), a pure pyroxenite source is generally incompatible with other global OIB (e.g., Dasgupta et al., 2010; Herzberg, 2011) and is not supported by the major element compositions of the measured Samoan and Azores lavas relative to the model liquids (Fig. 7). The heaviest modelled pyroxenite melts are produced at low-degrees of melting, 13–14 kbar (∼50 km depth) and ∼1200°C (Fig. 6c & d). Plume geotherms are unlikely to intersect this part of the melting region, e.g., Azores melts are thought to form at > 1400°C and > 25 kbar (Beier et al., 2012); Samoa melts at > 1600°C and > 30 kbar (Putirka et al., 2018). Moreover, we expect mixing between pyroxenite and peridotite melts upon ascent in the mantle, even if pyroxenite melts first (Lambart et al., 2016). Therefore, pure,

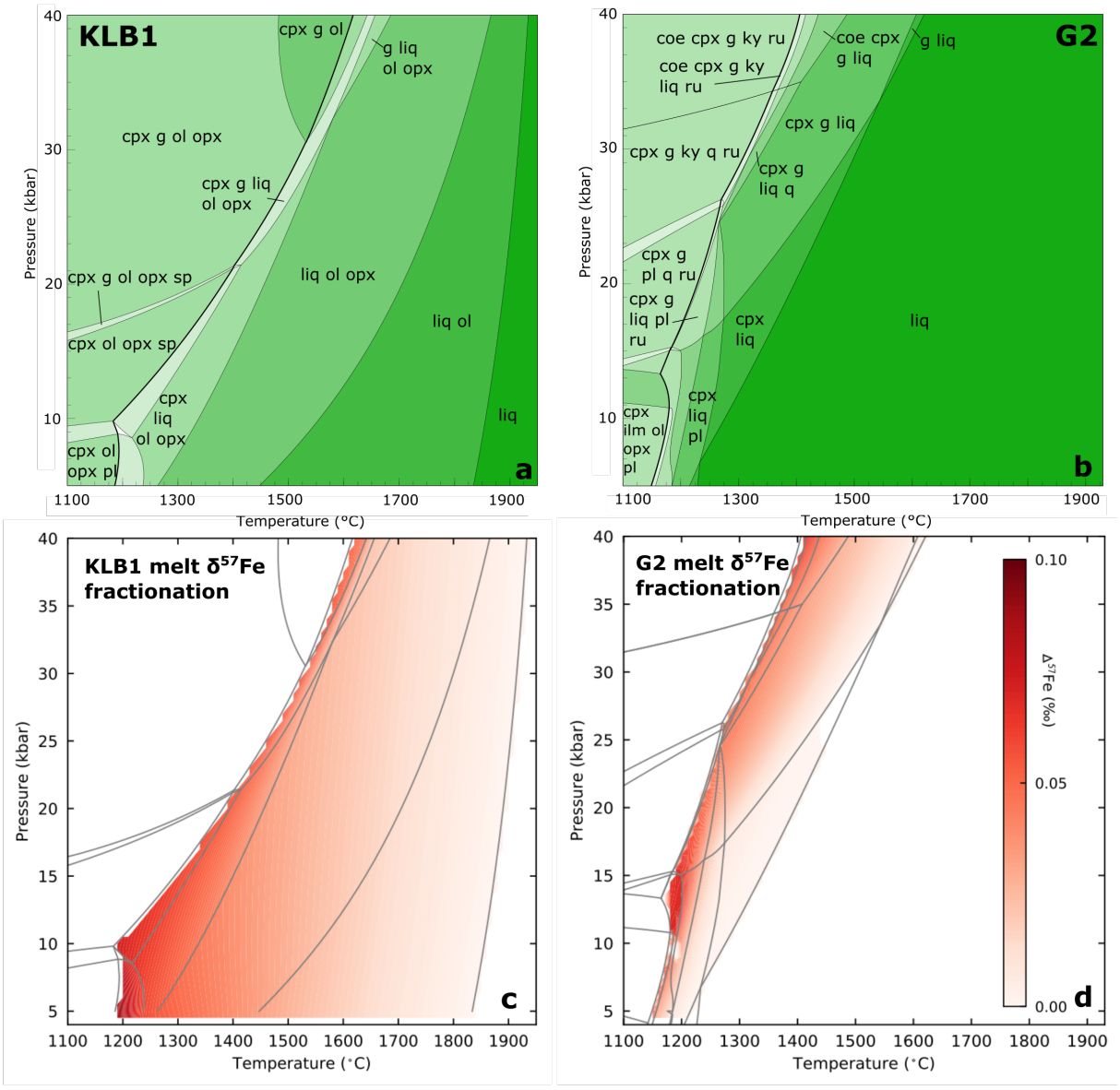

Figure 6: Results of the combined phase equilibria and isotope fractionation model for KLB1 and G2 lithologies. a, b show the stable mineral phases calculated using THERMOCALC, with the solidus highlighted in bold. c, d show the calculated partial melting fractionation from the pseudosections in a and b. The magnitude of the maximum partial melting Fe isotopic fractionation, Δ^{57}Fe, is small and independent of the bulk composition used.

heavy-δ^{57}Fe eclogitic pyroxenite melts are unlikely.

We also note that a contribution to a peridotite-dominated melt from an eclogitic pyroxenite melt could explain why average MORB, after correction for fractional crystallisation, sits at the heavier end of predicted KLB1 melt δ^{57}Fe compositions. An enriched, fertile lithology has been proposed previously to be a small, ubiquitously distributed component of the MORB source, to balance depleted components seen in abyssal peridotites (Salters and Dick, 2002; Byerly and Lassiter, 2014) and the garnet signature seen in trace elements in MORB (Hirschmann and Stolper, 1996). The Fe isotope data would be consistent with this enriched component being a refertilised peridotite (i.e., still an olivine-bearing lithology, but with more clinopyroxene than depleted mantle and a slightly elevated bulk δ^{57}Fe), or even a pyroxenite to match the heaviest MORB δ^{57}Fe compositions. Sun et al. (2020) record MORB glass samples from EPR seamounts with δ^{56}Fe $\leq$ 0.36‰ (δ^{57}Fe $\leq$ 0.54‰), where the high Fe isotope variability relative to average MORB is suggested to relate to limited melt mixing with ambient mantle in the seamounts compared to the ridge axis. The heavy δ^{57}Fe compositions are attributed to garnet pyroxenite veins in recycled, metasomatised oceanic lithosphere, processes which are discussed further in Section 5.4.

The modelled major element chemistry could be made more consistent with the Samoa and Azores lavas by changing the type of pyroxenite: SD pyroxenites, such as MIX1G (a composition resembling average natural SD pyroxenites, produced by mixing MORB with peridotite), produce melts with Al_2O_3 that overlap more OIB compositions than G2 (Hirschmann et al., 2003; Kogiso et al., 2003). In agreement with this, mixing the modelled KLB1 and G2 melts in Fig. 7 could produce melts that cover more of the OIB lava compositions than each individual lithology. However, pyroxenites generated by mixing MORB with peridotite would produce a bulk δ^{57}Fe lighter than G2 which, given the same $\Delta^{57}Fe_{melt-solid}$, would not be able to generate heavy δ^{57}Fe in OIB.

The isotopically heaviest Samoan shield and Azores melts, and all rejuvenated Samoan melts, are isotopically heavier than those produced from plausible conditions of a single-stage mixed peridotite–pyroxenite melting model.

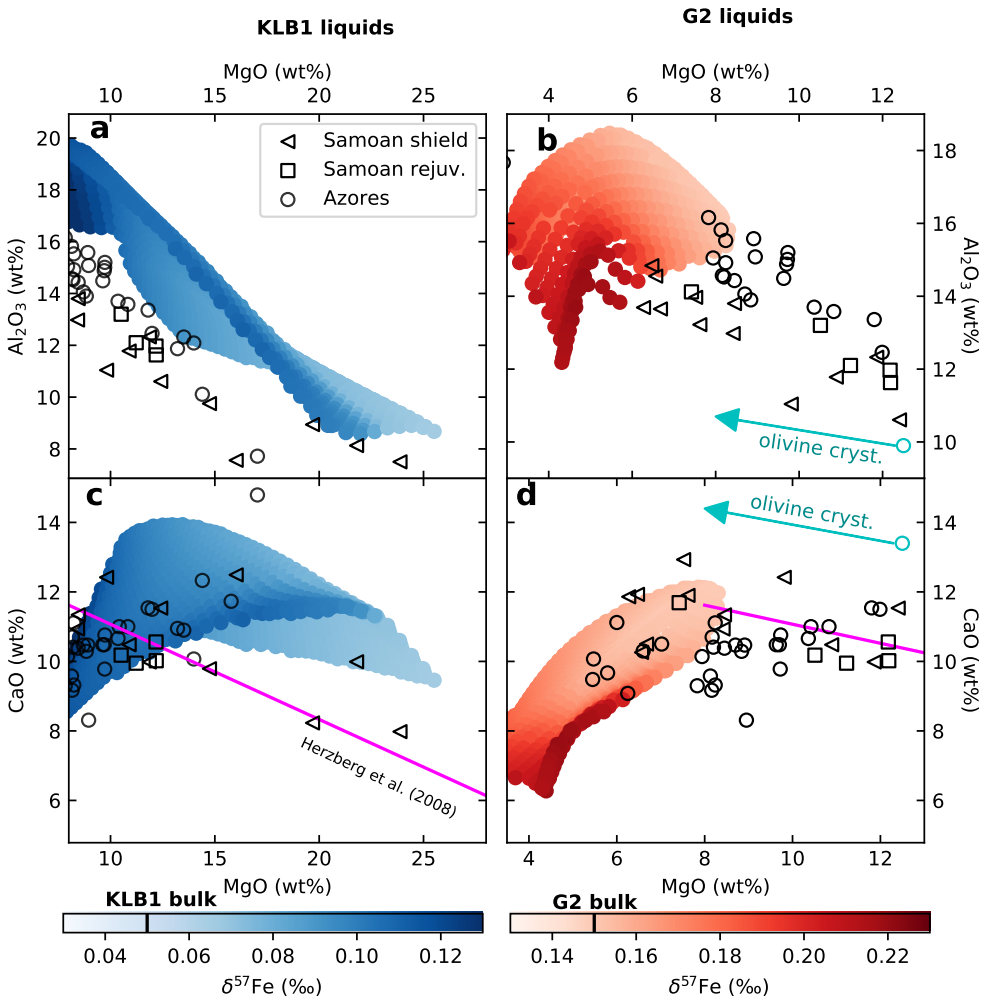

Figure 7: Coloured circles show the compositions of KLB1 (left) and G2 (right) melts produced in the model, coloured for δ^{57}Fe (KLB1 melts filtered for melt fraction $< 30\%$ to give a realistic MgO range). Samoa and Azores lavas are superimposed. Although pure pyroxenite melts are implied by the Fe isotopic composition, observed lava compositions are not consistent with pure pyroxenite melts. Pink line shows the separation of accumulated fractional melts from pyroxenite and peridotite source melts in CaO-MgO space from Herzberg and Asimow (2008) — peridotite source melts mostly plot above the line, pyroxenite melts mostly below. An example vector of melts related by olivine fractional crystallisation is shown.

5 How to generate heavy δ^{57}Fe mantle components?

The inability of a simple peridotite–eclogitic pyroxenite melting model (Section 4.2.3) to generate the heavy δ^{57}Fe of Samoa, Pitcairn and Azores melts means that pre-final melt emplacement processes (i.e., processes affecting the source δ^{57}Fe composition) must be considered. After core contributions, we sequentially consider processes operating from a mid-ocean ridge setting, through subduction, to upwelling and melting in a mantle plume (summarised in Fig. 8).

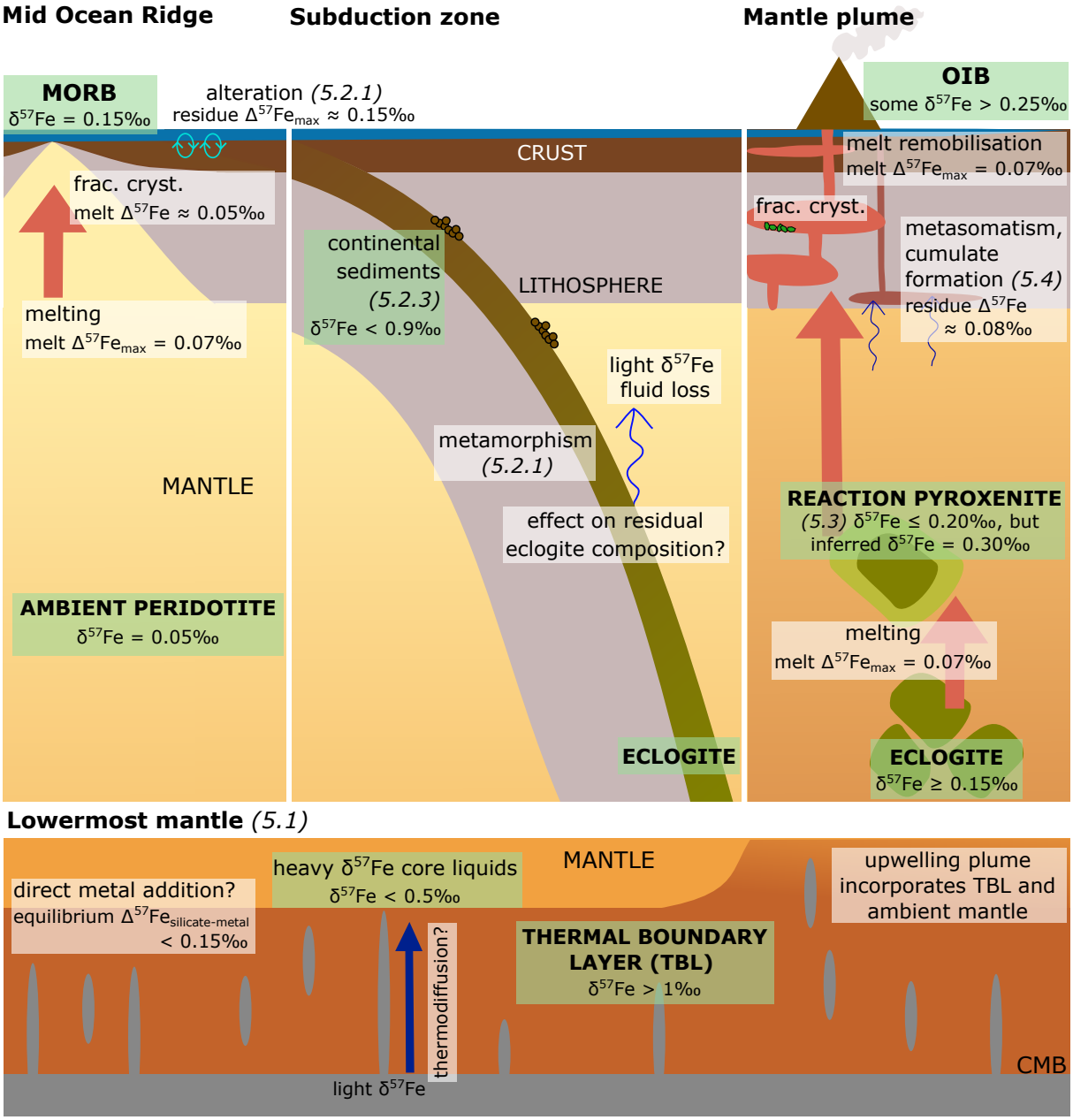

Figure 8: Schematic showing processes that may contribute to OIB liquids with heavier δ^{57}Fe than those predicted by single-stage melting of eclogite (Section 4.2.3). Processes including hydrothermal alteration (El Korh et al., 2017) and metamorphism (Debret et al., 2016) may increase subducted eclogite δ^{57}Fe (> 0.15‰), and the addition of continental sediments could contribute to recycled crustal domains with δ^{57}Fe > 0.15‰. Reaction pyroxenites have inferred δ^{57}Fe ≈ 0.30‰ from erupted lavas (Nebel et al., 2019; Gleeson et al., 2020), however generation of this component requires eclogite to have δ^{57}Fe significantly greater than 0.15‰ (Section 5.3). Metasomatism (Konter et al., 2016), fractional crystallisation and secondary melting may further contribute to heavy δ^{57}Fe ($>$ 0.25‰) liquids measured in OIB. Contributions from core liquids have also been proposed to generate heavy δ^{57}Fe in OIB (Lesher et al., 2020). Numbers in italics refer to the sections each process is discussed in.

5.1 Is heavy δ^{57}Fe a core component?

Many OIB are suggested to entrain lower mantle material. Short-lived radiogenic isotope systems and noble gases support that some OIB have incorporated small amounts of primordial, less-

degassed mantle material from the first 0.5 Ga of Earth's history, and/or core-equilibrated liquids, possibly stored near the CMB (e.g., Mukhopadhyay, 2012; Mundl et al., 2017; Peters et al., 2018; Rizo et al., 2019; Mundl-Petermeier et al., 2019, 2020). Calculated equilibrium silicate-metal fractionation factors at high pressures and temperatures are small ($\Delta^{57}Fe_{silicate-metal} \lesssim 0.15‰$; Polyakov, 2009; Shahar et al., 2016; Liu et al., 2017). Given that W and He isotope data support $< 0.3\%$ core-equilibrated material in OIB (Mundl-Petermeier et al., 2020), this small equilibrium fractionation is unlikely to contribute to heavy δ^{57}Fe in OIB. However, it has been proposed (Lesher et al., 2020) that heavy δ^{57}Fe in OIB could be generated by the incorporation of a kinetically-fractionated heavy δ^{57}Fe liquid iron and silicate layer from the lowermost mantle into an upwelling plume (Fig. 9). In this model, isotopic fractionation occurs by thermodiffusion (Soret diffusion), due to the relative motion of heavy and light isotopes in a liquid in response to a temperature gradient. In the case of liquid iron infiltrating the lowermost mantle near the CMB, heavy δ^{57}Fe migrates towards lower temperatures further from the CMB, forming a thin, heavy δ^{57}Fe ($< 0.5‰$, average $\approx 0.1‰$) boundary layer just above the CMB, which can be entrained by a rising mantle plume. As the plume rises, the core liquids freeze to preserve the isotopic anomaly, and the resultant plume is a mixture of this core component and ambient silicate mantle. This process produces a plume with average $\delta^{57}Fe > 0.05‰$ heavier than chondritic mantle depending on the core contribution (Lesher et al., 2020). The proposed average δ^{57}Fe offset of the plume relative to ambient mantle could explain part of the range of heavy δ^{57}Fe in OIB relative to MORB, so the process is discussed below, but the addition of the core liquids modelled by Lesher et al. (2020) still cannot explain the heaviest ($\delta^{57}Fe \gtrsim 0.25‰$) OIB lavas.

Heavy δ^{57}Fe in OIB generated from the core-contribution model should be linked to other geochemical signatures of core material: specifically, low $^{182}W/^{184}W$ (negative μ^{182}W) and high $^{3}He/^{4}He$ (Lesher et al., 2020), as well as high $^{186,187}Os/^{188}Os$, strong HSE enrichment (Brandon and Walker, 2005), and possibly high Fe/Mn (Humayun et al., 2004; Rizo et al., 2019). However, HSE enrichment in OIB that show negative μ^{182}W signatures is generally not observed (Mundl et al., 2017; Mundl-Petermeier et al., 2019), which could be attributed to the presence of a core-equilibrated reservoir rather than direct incorporation of core material providing the μ^{182}W signatures (Mundl-Petermeier et al., 2020).

The global OIB δ^{57}Fe dataset does not show a relationship between heavy δ^{57}Fe and volcanoes or plumes that show negative μ^{182}W and high ^{3}He/^{4}He, or high Fe/Mn (Fig. S5). The Samoan volcano of Ofu records ^{3}He/^{4}He $\leq$ 33.8 R/R$_a$ (Jackson et al., 2007a) and negative μ^{182}W ($\geq$ $-$17.3; Mundl et al., 2017; Mundl-Petermeier et al., 2020). However, the same Ofu samples measured here have δ^{57}Fe indistinguishable from MORB. This is inconsistent with the presence of frozen core liquid contributing to isotopically heavy δ^{57}Fe melts in the upwelling plume. There is a small negative μ^{182}W anomaly (and slightly raised Fe/Mn) recorded in the Azores plume as a whole (Rizo et al., 2019; Mundl-Petermeier et al., 2020), but Fe/Mn ratios for Pico (with a negative μ^{182}W; Rizo et al., 2019) show the least evidence of high-Fe in the Azores mantle, being similar to Icelandic lavas (Humayun et al., 2004; Qin and Humayun, 2008). The highest Fe/Mn ratio were measured in lavas from São Jorge (and São Miguel) that have not all been analysed for Fe or W isotopes (see Appendix, Table S4), but where samples have both Fe/Mn and δ^{57}Fe data there is no relationship between the two (Fig. S5). Other high ^{3}He/^{4}He lavas (e.g., Baffin) also show no heavy δ^{57}Fe anomaly relative to average MORB (McCoy-West et al., 2018), although this could be related to the high mantle potential temperatures associated with the Icelandic plume and plume head (Matthews et al., 2016; Spice et al., 2016) and therefore high degrees of melting of ambient peridotite. Overall, current data do not support a link between heavy δ^{57}Fe and the presence of core liquids entrained in an upwelling plume, and we instead consider modifications to the model of subducted, recycled material.

5.2 The Fe isotopic composition of subducted material

Pyroxenite melts that are isotopically heavier than the model melts shown in Fig. 4b, and therefore more consistent with measured OIB melts, could be generated if subducted material had δ^{57}Fe > 0.15‰. This heavy δ^{57}Fe could be caused by: (i) alteration of oceanic crust either hydrothermally at the seafloor, or during devolatilisation and metamorphism associated with subduction; (ii) ancient MORB being inherently isotopically heavier than modern MORB; or (iii) contributions from isotopically heavy subducted sediments.

5.2.1 Hydrothermal alteration and subduction processes

Studies of subduction zone metabasites suggest that hydrothermal alteration of basalt at shallow crustal levels could make subducted basalt isotopically heavier than MORB. For example, in Île de Groix, France (a HP-LT metamorphic belt), hydrothermal alteration makes subducted basalt isotopically heavier by Δ^{56}Fe = 0.06–0.10‰ (equivalent to Δ^{57}Fe = 0.09–0.15‰), contributing to the heavy Fe compositions of eclogites (δ^{57}Fe = 0.25–0.28‰; El Korh et al., 2017). Taking the maximum amount of Fe isotope variability attributed to hydrothermal alteration by El Korh et al. (2017), partial melts of hydrothermally altered crust could be as heavy as δ^{57}Fe = 0.37‰. Melting of this material, if present in mantle plumes, could explain the entire range of Samoan shield and Azores melts, and some of the rejuvenated Samoan liquids. Further geochemical studies, such as oxygen isotopes (Day et al., 2010), could help test the role of crustal alteration on heavy δ^{57}Fe. Alteration may also introduce sample heterogeneity, which could explain the different δ^{57}Fe found between this study and Konter et al. (2016) for sample ALIA115-18, and highlights that samples chosen for Fe isotope analyses should be carefully picked (due to this heterogeneity, the sample is not included in Figs. 2, 3, 4 & 5). However, Rouxel et al. (2003) showed that on a scale larger than a few metres, bulk hydrothermally altered oceanic crust is indistinguishable in δ^{57}Fe from MORB.

Therefore, the ability of hydrothermal alteration to generate large scale heavy δ^{57}Fe recycled crustal domains in the mantle remains uncertain, but is likely small. Any contribution from hydrothermally altered MORB protolith to OIB melts may not be distinguishable in major element compositions, as large major element variability in altered basalts is only recorded where a large proportion of alteration (e.g., > 30% Fe^{2+} loss) has taken place (Rouxel et al., 2003).

Isotopically heavy mantle components could also be generated by metamorphic and/or devolatilisation reactions, driving metabasites to heavier δ^{57}Fe values than their protolith. For example, Île de Groix blueschists have heavy δ^{57}Fe (0.26–0.51‰; El Korh et al., 2017), which could be partly explained by the loss of isotopically light fluids during prograde metamorphism: progressive serpentinite devolatilisation in the Western Alps records an increase of $\Delta^{56}Fe_{blueschist-serpentinite}$ = 0.12‰ (Δ^{57}Fe = 0.18‰) from abyssal serpentinites to blueschists

(Debret et al., 2016). Increasing δ^{57}Fe with devolatilisation is ascribed to loss of Fe(II)-Cl or Fe(II)-S complexes in serpentinite-derived fluids (Debret et al., 2016), which is consistent with light δ^{57}Fe in secondary olivines precipitated from serpentinite fluids (Debret et al., 2018). Infiltration by isotopically light slab-derived fluids have also been proposed to explain light (δ^{57}Fe < 0‰) peridotite fragments observed above the Philippine arc (Turner et al., 2018).

However, the origin of heavy δ^{57}Fe in Île de Groix blueschists is unclear, with El Korh et al. (2017) suggesting that much of the variability is likely to have been inherited from the original protolith, rather than generated during subduction. Studies have also shown that Fe is not fractionated in the downgoing oceanic crust during prograde metamorphism: orogenic eclogites preserve a MORB-like Fe isotope composition (δ^{57}Fe = 0.15‰; Williams et al., 2009; Li et al., 2016); Western Alpine eclogites also record no Fe isotope fractionation from MORB δ^{57}Fe, despite evidence from associated metagabbros of infiltration by a light δ^{57}Fe fluid (Inglis et al., 2017). Preserved eclogite MORB-like δ^{57}Fe could be the result of mass balance between the slab and fluid, leaving no resolvable Fe isotope heterogeneity after fluid loss in the subducted, dehydrated eclogitic material. The role of the loss of slab-derived fluids on the Fe isotopic composition of subducted material is further complicated by sources of fluids other than serpentinites, such as fluids derived from the altered oceanic crust, which could have heavy δ^{57}Fe as heavy δ^{57}Fe hydrous minerals (e.g., amphibole, epidote) break down (Huang et al., 2020).

5.2.2 The composition of ancient MORB

While the Fe isotopic composition of modern oceanic crust is well-studied, the material that now contributes to mantle heterogeneity may have been subducted more than a billion years ago (Montanini and Tribuzio, 2015). If ancient oceanic crust was isotopically heavier than the modern equivalent, it may have contributed to the formation of heavy δ^{57}Fe mantle domains sampled by OIB. Factors introducing temporal variability in the bulk isotopic composition of oceanic crust could be: (i) isotopic fractionation during partial melting and fractional crystallisation; and (ii) the amount and/or isotopic effect of hydrothermal alteration.

Magnitude of isotopic fractionations: Isotopic fractionation during ancient mantle partial melting, and/or fractional crystallisation of the subsequent melts, would need to be greater than

modern values to generate oceanic crust with δ^{57}Fe > 0.15‰ from a silicate mantle with δ^{57}Fe similar to the present-day value. However, hotter average upper mantle temperatures in the past (Herzberg et al., 2010) argue against larger Δ^{57}Fe, both because equilibrium isotopic fractionation factors decrease with temperature (Urey, 1947) and partial melting fractionation is smaller at higher degrees of melting (Fig. 6). This relationship is consistent with komatiites, generally ascribed to high melting temperatures, recording an average δ^{57}Fe more similar to BSE than average terrestrial basalts (Hibbert et al., 2012; Johnson et al., 2020). Mantle fO_2 may also affect the composition of mantle melts due to varying Fe^{3+}/Fe_T over time (Williams et al., 2004), hence the crustal δ^{57}Fe composition. However, Hibbert et al. (2012) records no difference in δ^{57}Fe from komatiites from the late Archean to the Tertiary associated with a mantle fO_2 effect, which is in agreement with other work suggesting that the mantle oxidation state has remained approximately fixed since the Archean (e.g., Berry et al., 2008).

Ancient hydrothermal alteration: Different processes operating in ancient hydrothermal systems compared to modern MORB could have contributed to δ^{57}Fe variability in subducted crust. Whereas modern hydrothermal systems generally precipitate more light δ^{57}Fe sulphides (e.g., Rouxel et al., 2004) than heavy δ^{57}Fe oxides, Precambrian hydrothermal systems precipitated fewer sulphides due to higher Fe/S and Fe^{2+} content in the fluids (Kump and Seyfried Jr, 2005). Therefore, Precambrian vent fluids may have precipitated dominantly heavy δ^{57}Fe minerals in the crust, and had lighter δ^{57}Fe than the present-day fluids (Johnson et al., 2020). However, even for modern hydrothermal systems, their influence on bulk altered crust δ^{57}Fe remains uncertain (Section 5.2.1), and so it is not possible to discern whether or not ancient hydrothermal systems could have generated heavier δ^{57}Fe in altered MORB than today.

5.2.3 Contributions from sediments

Subducted slab material includes oceanic lithosphere, crust, and sediments. Downgoing sediments are suggested to contribute to mantle heterogeneity (White and Hofmann, 1982; Plank and Langmuir, 1998), with small amounts of continental sediments traced in enriched mantle reservoirs ($\leq 10\%$; e.g., Jackson et al., 2007b; Rapp et al., 2008). Continental sediments could contribute to heavy δ^{57}Fe mantle domains, since differentiated igneous rocks record variable δ^{57}Fe (≤ 0.9‰; Du et al., 2017). However, bulk upper continental crust (the main component of

recycled sediment in the mantle; Stracke, 2012), is thought to be isotopically indistinguishable from MORB (Johnson et al., 2020), and direct measurements of arc system sediments show δ^{57}Fe = 0.17‰ (Nebel et al., 2015). Moreover, large-scale sediment input into the mantle is not expected because most sediment is scraped off in the forearc and never subducted; much of the sediment that does subduct may melt early and be returned to the surface in arc volcanism (Jackson et al., 2007b).

The Vai (weak HIMU) and Malu (EM2; Jackson et al., 2014) trends in Samoa, as distinguished in radiogenic isotope space (Fig. 1), are proposed to reflect the sampling of different mantle heterogeneities, including sediments. These heterogeneities may originate from different recycled material, explaining their radiogenic isotopic differences, hence might be expected to show δ^{57}Fe variability related to the recycled material. However, the melts of any recycled mantle component (e.g., sediments, oceanic crust) are likely to be mixed with ambient peridotite melts during shield stage volcanism. Since the contribution of Fe from non-peridotitic components will not dominate the Fe content of melts (unlike incompatible radiogenic isotopes), mass balance would argue against small fractions of non-peridotitic components in the mantle source being resolved using δ^{57}Fe where melt fraction is sufficiently high for peridotite melts to dominate. The Fe isotopic composition of melts is dependent on both mantle processes and source lithology and, in this case, processing rather than source composition may dominate melt δ^{57}Fe — small variations in the δ^{57}Fe of isotopically heavy melts from dilute HIMU and EM2 components may be eliminated by mixing with isotopically light peridotite melts.

5.3 Generating pyroxenites by peridotite hybridisation

In existing studies, the proposed formation of a solid pyroxenite component in the mantle that contributes to melts in OIB (e.g., the Pitcairn EM1 mantle component; Nebel et al., 2019) is a two-stage process, rather than only eclogite subduction and recycling. Reaction-zone pyroxenite is proposed to form by the reaction of high pressure (> 30 kbar) Si-rich melts from recycled oceanic crust with ambient peridotite, producing an olivine-free hybrid pyroxenite lithology (Sobolev et al., 2005, 2007; Rosenthal et al., 2014; Nebel et al., 2019; Fig. 9), which is suggested to have δ^{57}Fe = 0.30‰ based on measured OIB data (Nebel et al., 2019; Gleeson et al., 2020). Here we examine whether our modelled eclogite melts can generate this heavy pyroxenite mantle

component.

Based on a single-stage melting process (Section 4.2.1), the heaviest melts that can be formed from subducted oceanic crust (with bulk δ^{57}Fe = 0.15‰) have δ^{57}Fe = 0.22‰. Mixing of these melts with peridotite (δ^{57}Fe = 0.05‰) would produce a lithology of δ^{57}Fe = 0.05–0.22‰, assuming equilibrium fractionation and depending on the proportion of eclogite melt involved. Remelting of this component could then produce liquids heavy enough to explain the isotopic compositions of Samoan shield and some of the Azores melts, but would require: (i) the solid reaction-zone pyroxenite to have an isotopic composition close to that of the Si-rich eclogite melt (maximum δ^{57}Fe = 0.22‰), and (ii) that pyroxenite melt (with δ^{57}Fe up to 0.29‰, taking the upper limit of melting fractionation from Section 4.2.1) was extracted without mixing with ambient peridotite melts (Fig. 9). It is also likely that the subsequent melts would have major element compositions similar to G2 melts and therefore not match the OIB major element geochemistry. Overall, this process cannot generate a sufficiently isotopically heavy solid mantle component to match previous estimates of pyroxenite composition (δ^{57}Fe $\geq$ 0.30‰; Nebel et al., 2019), nor subsequently produce the heaviest observed OIB melt compositions. Instead, forming pyroxenite by hybridisation produces a range of subsequent melt compositions likely dominated by δ^{57}Fe similar to MORB, but could produce some heavier δ^{57}Fe melts that contribute to the heavy δ^{57}Fe seen in OIB.

5.4 Lithospheric processing and remobilisation

Remobilisation of small-degree pyroxenite melts, frozen in the lithosphere during the passage of the main plume head, could generate liquids isotopically heavier than those from a single-stage mantle melting process. Melt remobilisation superimposes a further partial melting fractionation of Δ^{57}Fe $\leq$ 0.07‰ onto the resultant melts, which are likely to be small-degree melts. Therefore, partial melting fractionations may be at the upper limit of the melting fractionation range; and minimal melting of, and thus minimal dilution by, isotopically light peridotite is expected. If the heaviest possible reaction-zone pyroxenite melts (δ^{57}Fe = 0.29‰; Fig. 9) could become trapped in the lithosphere and subsequently remobilised, it would be possible to generate small-degree melts with δ^{57}Fe $\lesssim$ 0.35‰. These melts could explain some of the rejuvenated Samoan lavas, since the Samoan lithosphere has previously passed over at least two hotspots (Jackson et al.,

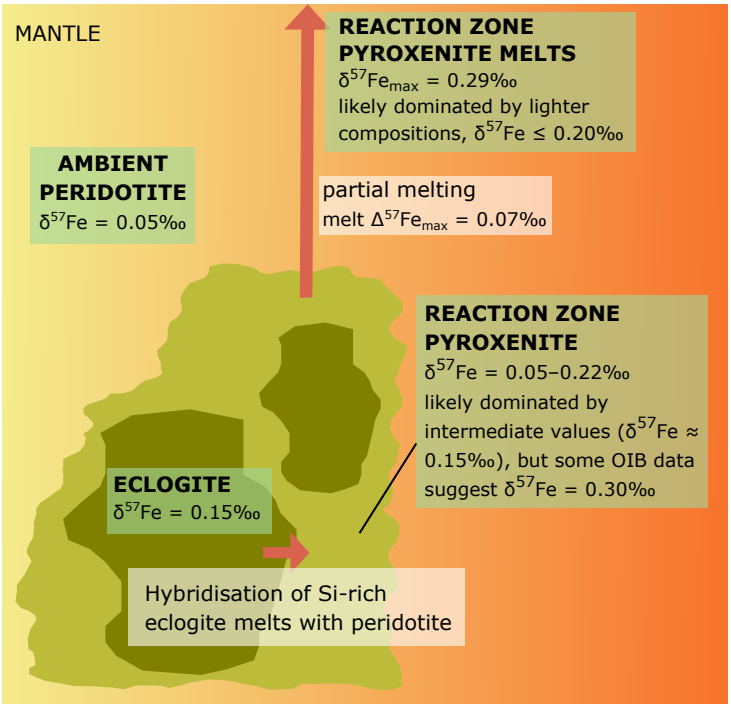

Figure 9: Schematic showing formation of a reaction zone pyroxenite, following Sobolev et al. (2005); Nebel et al. (2019), and the subsequent generation of heavy δ^{57}Fe melts. Eclogite melts hybridise with ambient peridotite, generating a pyroxenite mantle component with $\delta^{57}\text{Fe} \leq 0.22‰$, assuming a subducted eclogite composition of $\delta^{57}\text{Fe} = 0.15‰$.

2010) so is likely to contain trapped veins of melt. The rejuvenated lavas have been proposed to be small-degree melts remobilised by decompression melting due to plate flexure near the Tonga trench, consistent with their low SiO_2, alkalic nature relative to shield samples, and may be an expression of 'petit spot' volcanism (Hawkins Jr and Natland, 1975; Natland, 1980; Konter and Jackson, 2012; Reinhard et al., 2019). However, erupted melts with compositions close to δ^{57}Fe = 0.35‰ would require that: (i) reaction-zone pyroxenite melts were extracted through two partial melting events without mixing with ambient peridotite melts, and (ii) at each melting stage, Fe isotopic fractionation was at a maximum ($\Delta^{57}\text{Fe} = 0.07‰$), despite the limited P-T conditions where this Δ^{57}Fe is possible (Fig. 6). In addition, to generate any large volume of small-degree, maximum Δ^{57}Fe melts requires a residual source that is much larger in mass than the melts for both melting events. This volume problem would make it difficult to generate appreciable quantities of eruptable heavy δ^{57}Fe melt, but it is possible that remobilisation of melts with less extreme melting Δ^{57}Fe (hence a smaller volume problem) could provide a small contribution to heavy δ^{57}Fe.

Metasomatic reactions of source peridotite with a melt or fluid, generating isotopic and chem-

ical disequilibrium and forming pyroxene-rich domains, may also be able to contribute to heavy isotopic signatures in OIB. Where metasomatism involves enrichment by a Fe-rich, Si-undersaturated melt (e.g., a silicate liquid that has evolved in mantle magma chambers and veins; Weyer and Ionov, 2007), formation of secondary clinopyroxene (as seen in some Samoan xenoliths; Finlayson et al., 2015) and generation of wehrlites (Ionov et al., 2005) could generate a heavy δ^{57}Fe metasomatised source (Weyer and Ionov, 2007; Konter et al., 2016). The precipitation of garnet and clinopyroxene at the interface between subsolidus lherzolite and eclogite-derived melts has also been shown experimentally and has occurred within the lithosphere of the North China Craton (Wang et al., 2020). Sun et al. (2020) proposes that metasomatic garnet pyroxenite veins in recycled oceanic lithosphere could melt and react with ambient peridotite to produce secondary pyroxenites with δ^{57}Fe > 0.3‰ although, as discussed in Section 5.3, it is unclear how these heavy compositions will be generated. Metasomatic phlogopite has also been recorded with heavy δ^{57}Fe in cratonic mantle xenoliths (> 0.30‰; Zhao et al., 2012), although Beier et al. (2012) argue against phlogopite in the Azores source on the basis of trace elements.

The suggested magnitude of the metasomatic effect, based on xenolith data from Samoa (Finlayson et al., 2015), is Δ^{56}Fe $= 0.05$‰ (Δ^{57}Fe $= 0.08$‰; Konter et al., 2016), which cannot generate the full δ^{57}Fe range of liquids observed in Samoa, but could contribute to producing heavy δ^{57}Fe. Some mantle samples affected by metasomatism record a strong negative correlation between δ^{56}Fe and δ^{26}Mg, which is consistent with an inter-diffusion disequilibrium origin to the isotopic signatures (Zhao et al., 2012; Su et al., 2015), and likely due to coupled diffusion into/out of mantle minerals. Therefore, Mg isotopic measurements might be able to identify heavy Fe isotopic signatures of a metasomatic origin, which could be particularly applicable for rejuvenated Samoan lavas (Konter et al., 2016).

Some SD pyroxenites are suggested to be lithospheric cumulates from low-degree mantle melts, e.g., some Hawaiian pyroxenite xenoliths, which have δ^{57}Fe ≤ 0.27‰ (Bizimis et al., 2013; Williams and Bizimis, 2014). These compositions have been explained by the progressive fractional crystallisation in the lithosphere of an initial melt with δ^{57}Fe $= 0.15$‰. However, the heaviest δ^{57}Fe xenolith is required to be a cumulate fraction in equilibrium with a highly evolved ($> 90\%$ fractionally crystallised) melt (Williams and Bizimis, 2014). For major elements, cumulate pyroxenite compositions can produce primary magmas that have higher CaO than eclogite-

derived melts, plotting above the dividing line in Fig. 7 (Herzberg and Asimow, 2008), although this CaO enriched composition would be inconsistent with the major element chemistry of most of the Azores and Samoan lavas shown here. Therefore, while xenoliths record the presence of heavy δ^{57}Fe (> 0.25‰) lithospheric components, their mode of formation and relevance to heavy δ^{57}Fe in OIB, particularly large-volume melts, remains uncertain.

The pre-final melting processes that have been discussed are summarised in Table 2, highlighting key points about the possibility of each consideration in explaining δ^{57}Fe of melts.

Table 2: Summary of processes that are discussed to contribute to heavy δ^{57}Fe melts in OIB. We consider the potential effects on melt δ^{57}Fe, in addition to major elements; and potential melt volume generated from this contribution to mantle heterogeneity, to identify plausible processes that are traced by δ^{57}Fe in OIB melts.

	Contribution to:			
Process	δ^{57}Fe	Major elements	Melt volume	Section
Core contribution	> 0.05‰ heavier than silicate mantle but not consistent with other isotopes	No difference	Could be mixed into whole plume to some extent	5.1
Make eclogite δ^{57}Fe > 0.15‰ by:				
(i) Hydrothermal alteration of oceanic crust	Bulk effect suggested to be small	Large variability only from highly altered protolith	Could be large component	5.2.1
(ii) Metamorphism and/or dehydration of subducted basalt	Bulk effect uncertain, could be small due to mass balance in slab	Likely small due to mass balance in slab	Could be large component	5.2.1
(iii) Composition of ancient MORB	Poorly constrained, but likely negligible	Poorly constrained	Could be large component	5.2.2
(iv) Sediment input to the mantle	Sediments ≤ 0.9‰, but bulk effect could be small	Bulk effect likely small	Likely small	5.2.3
Generate reaction-zone pyroxenites	Melts ≤ 0.29‰, likely closer to 0.15‰	Mix between peridotite and pyroxenite melt compositions	Could be large component	5.3
Lithospheric processing				
(i) Melt remobilisation	Superimposes a further $\Delta^{57}Fe_{max} = 0.07$‰	Small-degree OIB melts likely alkalic	Likely small	5.4
(ii) Metasomatism	Could increase melt δ^{57}Fe due to pyroxene enrichment	Measurable e.g., CaO enrichment	Likely small	5.4

6 Preservation of heavy δ^{57}Fe: Importance of plume variables

Not all OIB record heavy δ^{57}Fe (e.g., Hawai'i, Samoan shield, Réunion), which suggests that the processes controlling the generation and preservation of heavy δ^{57}Fe in erupted lavas may rely

on factors that differ between plumes, e.g., melt fraction and potential temperature, in addition to the δ^{57}Fe of source material.

The Azores records heavy δ^{57}Fe and is a relatively cool plume (Putirka, 2008; Beier et al., 2012), and the heavy δ^{57}Fe rejuvenated Samoan lavas are small-degree melts (Konter and Jackson, 2012). Therefore, heavy δ^{57}Fe melts may be more likely to be preserved in plumes where they are not diluted by extensive degrees of melting and/or mixing with ambient peridotite mantle melts, regardless of how a heavy δ^{57}Fe source component is generated. Hawai'i and Samoa have notably high excess temperatures, with a potential temperature anomaly of > 200°C (Putirka, 2005) compared to only 35°C in the Azores (Beier et al., 2012), and record no heavy δ^{57}Fe in erupted shield stage melts (Teng et al., 2008, 2013; Konter et al., 2016). However, a link between plume excess temperature and δ^{57}Fe is likely to be complicated by other factors affecting melt fraction, such as lithospheric thickness and mantle source components, and we note that some plumes (for example Réunion) with a similar excess temperature to Pitcairn (Putirka, 2008) have no measured heavy δ^{57}Fe lavas.

7 Summary

Stable Fe isotopes have increasingly been used as a tracer of mineralogical heterogeneity in the mantle, but there are multiple processes that could generate heavy δ^{57}Fe mantle melts. We show that the existing dataset of δ^{57}Fe, μ^{182}W and ^{3}He/^{4}He of OIB are inconsistent with a contribution from heavy δ^{57}Fe core liquids. In agreement with previous work, we also calculate that the magnitude of partial melting fractionation of peridotite is small. We show that the partial melting fractionation of an eclogitic pyroxenite is similar to that of peridotite, and less than that required to explain the heaviest δ^{57}Fe seen in basalts — therefore, heterogeneity in melt δ^{57}Fe derives from the bulk δ^{57}Fe of source lithologies. Mixed melts of KLB1 peridotite and G2 eclogitic pyroxenite (with bulk compositions of δ^{57}Fe = 0.05 and MORB-like 0.15‰ respectively) produce liquids that match some of the Samoan shield and Azores melts, but would need to comprise nearly pure pyroxenite melts to explain the heaviest δ^{57}Fe, and cannot explain any of the rejuvenated Samoan samples.

We show that to produce a mantle source capable of generating melts that match the OIB δ^{57}Fe

range requires consideration of processes operating from MORB generation, through mantle heterogeneity development and lithospheric processing, to eruption at ocean islands. The dominant contributor to geochemical heterogeneity recorded in OIB is recycled oceanic crust, which could generate heavy δ^{57}Fe ($\gtrsim 0.2$‰) melts if recycled crust was heavier in δ^{57}Fe than modern MORB (> 0.15‰). Heavy δ^{57}Fe in recycled material could be created by hydrothermal alteration, metamorphic reactions during subduction, or Fe isotope contributions from sediments, but we suggest no single, unique factor can explain the heaviest OIB δ^{57}Fe (> 0.25‰) lavas. Reaction-zone pyroxenites in the mantle, formed by the hybridisation of modelled equilibrium eclogitic melts and peridotite, will not be sufficiently isotopically heavy to match the proposed heavy δ^{57}Fe mantle component beneath Pitcairn and the Galapagos (Nebel et al., 2019; Gleeson et al., 2020), unless eclogite in the mantle has δ^{57}Fe > 0.15‰, i.e., has been modified from MORB values. Further processes contributing to heavy δ^{57}Fe melts could include the formation of isotopically heavy metasomatic pyroxene-rich domains and cumulates in the lithosphere, which may be remelted during late stages of plume activity (such as small-scale rejuvenated volcanism).

Any heavy δ^{57}Fe mantle or lithospheric component may most likely be observed in erupted lavas where overall melt volume and/or degree of melting is small, e.g., plumes with relatively low potential temperature. The measurement of MORB-like δ^{57}Fe signatures in an ocean island system therefore does not rule out the presence of a heavy δ^{57}Fe component in the mantle, as melts derived from this component may be too dilute in the erupted liquid to be distinguished by Fe isotopes.

Heavy δ^{57}Fe in OIB may have an important role to play in identifying mantle source lithologies, but the presence or absence of a heavy δ^{57}Fe signature in melts is unlikely to simply relate to a uniform recycled component in the mantle. Instead, Fe isotopes in OIB reflect a variety of often poorly-understood, difficult-to-distinguish and plume-specific processes that have contributed to variable δ^{57}Fe in the mantle and erupted melts.

Acknowledgements

We thank Edward Inglis and Geoff Nowell for their help in the labs in Durham, and Marie-Laure Bagard for her help with mass spectrometry in Cambridge. M. H. thanks Luisa Pinto Ribeiro (EMEPC, Lisbon) for the São Jorge samples (SJ48-101). We thank William Miller for valuable discussions and comments throughout this project; Bradley Peters, James Day, and an anonymous reviewer for useful comments that improved the clarity and focus of the manuscript; and Stefan Weyer for editorial handling. This work was supported by a NERC Studentship NE/L002507/1 to C.R.S., and ERC Consolidator Grant 306655 'HabitablePlanet' and NERC Consortia Grant ('Mantle Reservoirs, volumes and fluxes' NE/M000303/1) to H.M.W.

References

Béguelin, P., Bizimis, M., Beier, C. and Turner, S. (2017), 'Rift–plume interaction reveals multiple generations of recycled oceanic crust in Azores lavas', *Geochimica et Cosmochimica Acta* **218**, 132–152.

Beier, C., Haase, K. M., Abouchami, W., Krienitz, M.-S. and Hauff, F. (2008), 'Magma genesis by rifting of oceanic lithosphere above anomalous mantle: Terceira Rift, Azores', *Geochemistry, Geophysics, Geosystems* **9**(12).

Beier, C., Haase, K. M. and Brandl, P. A. (2018), Melting and mantle sources in the Azores, *in* 'Volcanoes of the Azores', Springer, pp. 251–280.

Beier, C., Haase, K. M. and Turner, S. P. (2012), 'Conditions of melting beneath the Azores', *Lithos* **144**, 1–11.

Beier, C., Mata, J., Stöckhert, F., Mattielli, N., Brandl, P. A., Madureira, P., Genske, F. S., Martins, S., Madeira, J. and Haase, K. M. (2013), 'Geochemical evidence for melting of carbonated peridotite on Santa Maria Island, Azores', *Contributions to Mineralogy and Petrology* **165**(5), 823–841.

Beier, C., Stracke, A. and Haase, K. M. (2007), 'The peculiar geochemical signatures of São Miguel (Azores) lavas: Metasomatised or recycled mantle sources?', *Earth and Planetary Science Letters* **259**(1-2), 186–199.

Beier, C., Turner, S., Plank, T. and White, W. (2010), 'A preliminary assessment of the symmetry of source composition and melting dynamics across the Azores plume', *Geochemistry, Geophysics, Geosystems* **11**(2).

Berry, A. J., Danyushevsky, L. V., O'Neill, H. S. C., Newville, M. and Sutton, S. R. (2008), 'Oxidation state of iron in komatiitic melt inclusions indicates hot Archaean mantle', *Nature* **455**(7215), 960–963.

Bizimis, M., Salters, V. J. M., Garcia, M. O. and Norman, M. D. (2013), 'The composition and distribution of the rejuvenated component across the Hawaiian plume: Hf-Nd-Sr-Pb isotope systematics of Kaula lavas and pyroxenite xenoliths', *Geochemistry, Geophysics, Geosystems* **14**(10), 4458–4478.

Brandon, A. D. and Walker, R. J. (2005), 'The debate over core–mantle interaction', *Earth and Planetary Science Letters* **232**(3-4), 211–225.

Brandon, A. D., Walker, R. J., Morgan, J. W., Norman, M. D. and Prichard, H. M. (1998), 'Coupled 186Os and 187Os evidence for core-mantle interaction', *Science* **280**(5369), 1570–1573.

Burton, K. W., Cenki-Tok, B., Mokadem, F., Harvey, J., Gannoun, A., Alard, O. and Parkinson, I. J. (2012), 'Unradiogenic lead in Earth's upper mantle', *Nature Geoscience* **5**(8), 570–573.

Byerly, B. L. and Lassiter, J. C. (2014), 'Isotopically ultradepleted domains in the convecting upper mantle: Implications for MORB petrogenesis', *Geology* **42**(3), 203–206.

Chauvel, C., Hofmann, A. W. and Vidal, P. (1992), 'HIMU-EM: the French Polynesian connection', *Earth and Planetary Science Letters* **110**(1-4), 99–119.

Cheng, T., Nebel, O., Sossi, P. A. and Chen, F. (2014), 'Refined separation of combined Fe–Hf from rock matrices for isotope analyses using AG-MP-1M and Ln-Spec chromatographic extraction resins', *MethodsX* **1**, 144–150.

Cohen, R. S. and O'Nions, R. K. (1982), 'Identification of recycled continental material in the mantle from Sr, Nd and Pb isotope investigations', *Earth and Planetary Science Letters* **61**(1), 73–84.

Cottrell, E. and Kelley, K. A. (2013), 'Redox heterogeneity in mid-ocean ridge basalts as a function of mantle source', *Science* **340**(6138), 1314–1317.

Craddock, P. R. and Dauphas, N. (2010), 'Iron Isotopic Compositions of Geological Reference Materials and Chondrites', *Geostandards and Geoanalytical Research* **35**(1), 101–123.

Craddock, P. R., Warren, J. M. and Dauphas, N. (2013), 'Abyssal peridotites reveal the near-chondritic Fe isotopic composition of the Earth', *Earth and Planetary Science Letters* **365**, 63–76.

Dasgupta, R., Hirschmann, M. M., McDonough, W. F., Spiegelman, M. and Withers, A. C. (2009), 'Trace element partitioning between garnet lherzolite and carbonatite at 6.6 and 8.6 GPa with applications to the geochemistry of the mantle and of mantle-derived melts', *Chemical Geology* **262**(1-2), 57–77.

Dasgupta, R., Jackson, M. G. and Lee, C.-T. A. (2010), 'Major element chemistry of ocean island basalts—conditions of mantle melting and heterogeneity of mantle source', *Earth and Planetary Science Letters* **289**(3-4), 377–392.

Dauphas, N., Craddock, P. R., Asimow, P. D., Bennett, V. C., Nutman, A. P. and Ohnenstetter, D. (2009), 'Iron isotopes may reveal the redox conditions of mantle melting from Archean to Present', *Earth and Planetary Science Letters* **288**(1-2), 255–267.

Dauphas, N., Roskosz, M., Alp, E. E., Neuville, D., Hu, M. Y., Sio, C. K., Tissot, F. L. H., Zhao, J., Tissandier, L., Médard, E. et al. (2014), 'Magma redox and structural controls on iron isotope variations in Earth's mantle and crust', *Earth and Planetary Science Letters* **398**, 127–140.

Davis, F. A., Tangeman, J. A., Tenner, T. J. and Hirschmann, M. M. (2009), 'The composition of KLB-1 peridotite', *American Mineralogist* **94**(1), 176–180.

Day, J. M. D., Pearson, D. G., Macpherson, C. G., Lowry, D. and Carracedo, J.-C. (2009), 'Pyroxenite-rich mantle formed by recycled oceanic lithosphere: Oxygen-osmium isotope evidence from Canary Island lavas', *Geology* **37**(6), 555–558.

Day, J. M. D., Pearson, D. G., Macpherson, C. G., Lowry, D. and Carracedo, J. C. (2010), 'Evidence for distinct proportions of subducted oceanic crust and lithosphere in HIMU-type mantle beneath El Hierro and La Palma, Canary Islands', *Geochimica et Cosmochimica Acta* **74**(22), 6565–6589.

Debret, B., Bouilhol, P., Pons, M. L. and Williams, H. (2018), 'Carbonate transfer during the onset of slab devolatilization: new insights from Fe and Zn stable isotopes', *Journal of Petrology* **59**(6), 1145–1166.

Debret, B., Millet, M.-A., Pons, M.-L., Bouilhol, P., Inglis, E. and Williams, H. (2016), 'Isotopic evidence for iron mobility during subduction', *Geology* **44**(3), 215–218.

Du, D.-H., Wang, X.-L., Yang, T., Chen, X., Li, J.-Y. and Li, W. (2017), 'Origin of heavy Fe isotope compositions in high-silica igneous rocks: a rhyolite perspective', *Geochimica et Cosmochimica Acta* **218**, 58–72.

Eisele, J., Sharma, M., Galer, S. J. G., Blichert-Toft, J., Devey, C. W. and Hofmann, A. W. (2002), 'The role of sediment recycling in EM-1 inferred from Os, Pb, Hf, Nd, Sr isotope and trace element systematics of the Pitcairn hotspot', *Earth and Planetary Science Letters* **196**(3-4), 197–212.

El Korh, A., Luais, B., Deloule, E. and Cividini, D. (2017), 'Iron isotope fractionation in subduction-related high-pressure metabasites (Ile de Groix, France)', *Contributions to Mineralogy and Petrology* **172**(6), 41.

Elliott, T., Blichert-Toft, J., Heumann, A., Koetsier, G. and Forjaz, V. (2007), 'The origin of enriched mantle beneath São Miguel, Azores', *Geochimica et Cosmochimica Acta* **71**(1), 219–240.

Farley, K. A., Natland, J. H. and Craig, H. (1992), 'Binary mixing of enriched and undegassed (primitive?) mantle components (He, Sr, Nd, Pb) in Samoan lavas', *Earth and Planetary Science Letters* **111**(1), 183–199.

Finlayson, V. A., Konter, J. G. and Ma, L. (2015), 'The importance of a Ni correction with ion counter in the double spike analysis of Fe isotope compositions using a 57Fe/58Fe double spike', *Geochemistry, Geophysics, Geosystems* **16**(12), 4209–4222.

Gale, A., Dalton, C. A., Langmuir, C. H., Su, Y. and Schilling, J.-G. (2013), 'The mean composition of ocean ridge basalts', *Geochemistry, Geophysics, Geosystems* **14**(3), 489–518.

Genske, F. S., Beier, C., Stracke, A., Turner, S. P., Pearson, N. J., Hauff, F., Schaefer, B. F. and Haase, K. M. (2016), 'Comparing the nature of the western and eastern Azores mantle', *Geochimica et Cosmochimica Acta* **172**, 76–92.

Gleeson, M. L. M. and Gibson, S. A. (2019), 'Crustal controls on apparent mantle pyroxenite signals in ocean-island basalts', *Geology* **47**(4), 321–324.

873 Gleeson, M. L. M., Gibson, S. A. and Williams, H. M. (2020), 'Novel insights from Fe-isotopes into the lithological
874 heterogeneity of Ocean Island Basalts and plume-influenced MORBs', *Earth and Planetary Science Letters* **535**.

875 Gonzaga, R. G., Lowry, D., Jacob, D. E., LeRoex, A., Schulze, D. and Menzies, M. A. (2010), 'Eclogites and garnet
876 pyroxenites: similarities and differences', *Journal of Volcanology and Geothermal Research* **190**(1-2), 235–247.

877 Hart, S. R. and Jackson, M. G. (2014), 'Ta'u and Ofu/Olosega volcanoes: The "Twin Sisters" of Samoa, their P,
878 T, X melting regime, and global implications', *Geochemistry, Geophysics, Geosystems* **15**(6), 2301–2318.

879 Hauri, E. H. and Hart, S. R. (1993), 'Re-Os isotope systematics of HIMU and EMII oceanic island basalts from
880 the south Pacific Ocean', *Earth and Planetary Science Letters* **114**(2-3), 353–371.

881 Hauri, E. H. and Hart, S. R. (1997), 'Rhenium abundances and systematics in oceanic basalts', *Chemical Geology*
882 **139**(1-4), 185–205.

883 Hauri, E. H., Shimizu, N., Dieu, J. J. and Hart, S. R. (1993), 'Evidence for hotspot-related carbonatite metaso-
884 matism in the oceanic upper mantle', *Nature* **365**(6443), 221–227.

885 Hawkins Jr, J. W. and Natland, J. H. (1975), 'Nephelinites and basanites of the Samoan linear volcanic chain:
886 Their possible tectonic significance', *Earth and Planetary Science Letters* **24**(3), 427–439.

887 Herzberg, C. (2011), 'Identification of source lithology in the Hawaiian and Canary Islands: Implications for
888 origins', *Journal of Petrology* **52**(1), 113–146.

889 Herzberg, C. and Asimow, P. D. (2008), 'Petrology of some oceanic island basalts: PRIMELT2. XLS software for
890 primary magma calculation', *Geochemistry, Geophysics, Geosystems* **9**(9).

891 Herzberg, C., Condie, K. and Korenaga, J. (2010), 'Thermal history of the Earth and its petrological expression',
892 *Earth and Planetary Science Letters* **292**(1-2), 79–88.

893 Hibbert, K. E. J., Williams, H. M., Kerr, A. C. and Puchtel, I. S. (2012), 'Iron isotopes in ancient and modern
894 komatiites: Evidence in support of an oxidised mantle from Archean to present', *Earth and Planetary Science*
895 *Letters* **321-322**, 198 – 207.

896 Hildenbrand, A., Weis, D., Madureira, P. and Marques, F. O. (2014), 'Recent plate re-organization at the Azores
897 Triple Junction: Evidence from combined geochemical and geochronological data on Faial, S. Jorge and Terceira
898 volcanic islands', *Lithos* **210**, 27–39.

899 Hirschmann, M. M., Kogiso, T., Baker, M. B. and Stolper, E. M. (2003), 'Alkalic magmas generated by partial
900 melting of garnet pyroxenite', *Geology* **31**(6), 481–484.

901 Hirschmann, M. M. and Stolper, E. M. (1996), 'A possible role for garnet pyroxenite in the origin of the "garnet
902 signature" in MORB', *Contributions to Mineralogy and Petrology* **124**(2), 185–208.

903 Hofmann, A. W. (1997), 'Mantle geochemistry: the message from oceanic volcanism', *Nature* **385**(6613), 219–229.

Hofmann, A. W. and White, W. M. (1982), 'Mantle plumes from ancient oceanic crust', *Earth and Planetary Science Letters* **57**(2), 421–436.

Hole, M. J. (2018), 'Mineralogical and geochemical evidence for polybaric fractional crystallization of continental flood basalts and implications for identification of peridotite and pyroxenite source lithologies', *Earth-Science Reviews* **176**, 51–67.

Holland, T. J. B., Green, E. C. R. and Powell, R. (2018), 'Melting of Peridotites through to Granites: A Simple Thermodynamic Model in the System KNCFMASHTOCr', *Journal of Petrology* **59**(5), 881–900.

Huang, J., Guo, S., Jin, Q.-Z. and Huang, F. (2020), 'Iron and magnesium isotopic compositions of subduction-zone fluids and implications for arc volcanism', *Geochimica et Cosmochimica Acta* **278**, 376–391.

Huang, S., Hall, P. S. and Jackson, M. G. (2011), 'Geochemical zoning of volcanic chains associated with Pacific hotspots', *Nature Geoscience* **4**(12), 874–878.

Humayun, M., Qin, L. and Norman, M. D. (2004), 'Geochemical evidence for excess iron in the mantle beneath Hawaii', *Science* **306**(5693), 91–94.

Inglis, E. C., Debret, B., Burton, K. W., Millet, M.-A., Pons, M.-L., Dale, C. W., Bouilhol, P., Cooper, M., Nowell, G. M., McCoy-West, A. J. et al. (2017), 'The behavior of iron and zinc stable isotopes accompanying the subduction of mafic oceanic crust: A case study from Western Alpine ophiolites', *Geochemistry, Geophysics, Geosystems* **18**(7), 2562–2579.

Ionov, D. A., Chanefo, I. and Bodinier, J.-L. (2005), 'Origin of Fe-rich lherzolites and wehrlites from Tok, SE Siberia by reactive melt percolation in refractory mantle peridotites', *Contributions to Mineralogy and Petrology* **150**(3), 335–353.

Jackson, M. G. and Dasgupta, R. (2008), 'Compositions of HIMU, EM1, and EM2 from global trends between radiogenic isotopes and major elements in ocean island basalts', *Earth and Planetary Science Letters* **276**(1-2), 175–186.

Jackson, M. G., Hart, S. R., Konter, J. G., Koppers, A. A., Staudigel, H., Kurz, M. D., Blusztajn, J. and Sinton, J. M. (2010), 'Samoan hot spot track on a "hot spot highway": Implications for mantle plumes and a deep Samoan mantle source', *Geochemistry, Geophysics, Geosystems* **11**(12).

Jackson, M. G., Hart, S. R., Konter, J. G., Kurz, M. D., Blusztajn, J. and Farley, K. A. (2014), 'Helium and lead isotopes reveal the geochemical geometry of the Samoan plume', *Nature* **514**(7522), 355–358.

Jackson, M. G., Hart, S. R., Koppers, A. A. P., Staudigel, H., Konter, J., Blusztajn, J., Kurz, M. and Russell, J. A. (2007b), 'The return of subducted continental crust in Samoan lavas', *Nature* **448**(7154), 684–687.

Jackson, M. G., Kurz, M. D., Hart, S. R. and Workman, R. K. (2007a), 'New Samoan lavas from Ofu Island reveal a hemispherically heterogeneous high $^{3}He/^{4}He$ mantle', *Earth and Planetary Science Letters* **264**(3-4), 360–374.

Johnson, C., Beard, B. and Weyer, S. (2020), High-Temperature Fe Isotope Geochemistry, *in* 'Iron Geochemistry: An Isotopic Perspective', Springer, pp. 85–147.

Johnson, C. M., Bell, K., Beard, B. L. and Shultis, A. I. (2010), 'Iron isotope compositions of carbonatites record melt generation, crystallization, and late-stage volatile-transport processes', *Mineralogy and petrology* **98**(1-4), 91–110.

Kogiso, T., Hirschmann, M. M. and Frost, D. J. (2003), 'High-pressure partial melting of garnet pyroxenite: possible mafic lithologies in the source of ocean island basalts', *Earth and Planetary Science Letters* **216**(4), 603–617.

Kogiso, T., Hirschmann, M. M. and Pertermann, M. (2004), 'High-pressure partial melting of mafic lithologies in the mantle', *Journal of Petrology* **45**(12), 2407–2422.

Konter, J. G., Hanan, B. B., Blichert-Toft, J., Koppers, A. A., Plank, T. and Staudigel, H. (2008), 'One hundred million years of mantle geochemical history suggest the retiring of mantle plumes is premature', *Earth and Planetary Science Letters* **275**(3-4), 285–295.

Konter, J. G. and Jackson, M. G. (2012), 'Large volumes of rejuvenated volcanism in Samoa: Evidence supporting a tectonic influence on late-stage volcanism', *Geochemistry, Geophysics, Geosystems* **13**(6).

Konter, J. G., Pietruszka, A. J., Hanan, B. B., Finlayson, V. A., Craddock, P. R., Jackson, M. G. and Dauphas, N. (2016), 'Unusual δ^{56} Fe values in Samoan rejuvenated lavas generated in the mantle', *Earth and Planetary Science Letters* **450**, 221–232.

Koppers, A. A. P., Russell, J. A., Roberts, J., Jackson, M. G., Konter, J. G., Wright, D. J., Staudigel, H. and Hart, S. R. (2011), 'Age systematics of two young en echelon Samoan volcanic trails', *Geochemistry, Geophysics, Geosystems* **12**(7).

Kump, L. R. and Seyfried Jr, W. E. (2005), 'Hydrothermal Fe fluxes during the Precambrian: Effect of low oceanic sulfate concentrations and low hydrostatic pressure on the composition of black smokers', *Earth and Planetary Science Letters* **235**(3-4), 654–662.

Lambart, S., Baker, M. B. and Stolper, E. M. (2016), 'The role of pyroxenite in basalt genesis: Melt-PX, a melting parameterization for mantle pyroxenites between 0.9 and 5 GPa', *Journal of Geophysical Research: Solid Earth* **121**(8), 5708–5735.

Lambart, S., Laporte, D. and Schiano, P. (2013), 'Markers of the pyroxenite contribution in the major-element compositions of oceanic basalts: Review of the experimental constraints', *Lithos* **160**, 14–36.

Larrea, P., França, Z., Widom, E. and Lago, M. (2018), Petrology of the Azores Islands, *in* 'Volcanoes of the Azores', Springer, pp. 197–249.

Larrea, P., Galé, C., Ubide, T., Widom, E., Lago, M. and França, Z. (2014), 'Magmatic evolution of Graciosa (Azores, Portugal)', *Journal of Petrology* **55**(11), 2125–2154.

Le Maitre, R. W., Streckeisen, A., Zanettin, B., Le Bas, M., Bonin, B. and Bateman, P. (2005), *Igneous rocks: a classification and glossary of terms: recommendations of the International Union of Geological Sciences Subcommission on the Systematics of Igneous Rocks*, Cambridge University Press.

Lesher, C. E., Dannberg, J., Barfod, G. H., Bennett, N. R., Glessner, J. J., Lacks, D. J. and Brenan, J. M. (2020), 'Iron isotope fractionation at the core–mantle boundary by thermodiffusion', *Nature Geoscience* pp. 1–5.

Li, D.-Y., Xiao, Y. L., Li, W.-Y., Zhu, X., Williams, H. M. and Li, Y.-L. (2016), 'Iron isotopic systematics of UHP eclogites respond to oxidizing fluid during exhumation', *Journal of Metamorphic Geology* **34**(9), 987–997.

Liu, C.-Z., Snow, J. E., Hellebrand, E., Brügmann, G., Von Der Handt, A., Büchl, A. and Hofmann, A. W. (2008), 'Ancient, highly heterogeneous mantle beneath Gakkel ridge, Arctic Ocean', *Nature* **452**(7185), 311–316.

Liu, J., Dauphas, N., Roskosz, M., Hu, M. Y., Yang, H., Bi, W., Zhao, J., Alp, E. E., Hu, J. Y. and Lin, J.-F. (2017), 'Iron isotopic fractionation between silicate mantle and metallic core at high pressure', *Nature communications* **8**(1), 1–6.

Maclennan, J. (2008), 'Lead isotope variability in olivine-hosted melt inclusions from Iceland', *Geochimica et Cosmochimica Acta* **72**(16), 4159–4176.

Macris, C. A., Manning, C. E. and Young, E. D. (2015), 'Crystal chemical constraints on inter-mineral Fe isotope fractionation and implications for Fe isotope disequilibrium in San Carlos mantle xenoliths', *Geochimica et Cosmochimica Acta* **154**, 168–185.

Madureira, P., Mata, J., Mattielli, N., Queiroz, G. and Silva, P. (2011), 'Mantle source heterogeneity, magma generation and magmatic evolution at Terceira Island (Azores archipelago): constraints from elemental and isotopic (Sr, Nd, Hf, and Pb) data', *Lithos* **126**(3-4), 402–418.

Matthews, S., Shorttle, O. and Maclennan, J. (2016), 'The temperature of the Icelandic mantle from olivine-spinel aluminum exchange thermometry', *Geochemistry, Geophysics, Geosystems* **17**(11), 4725–4752.

Matzen, A. K., Baker, M. B., Beckett, J. R., Wood, B. J. and Stolper, E. M. (2017), 'The effect of liquid composition on the partitioning of Ni between olivine and silicate melt', *Contributions to Mineralogy and Petrology* **172**(3).

McCoy-West, A. J., Fitton, J. G., Pons, M.-L., Inglis, E. C. and Williams, H. M. (2018), 'The Fe and Zn isotope composition of deep mantle source regions: Insights from Baffin Island picrites', *Geochimica et Cosmochimica Acta* **238**, 542–562.

Millet, M.-A., Doucelance, R., Baker, J. A. and Schiano, P. (2009), 'Reconsidering the origins of isotopic variations in Ocean Island Basalts: insights from fine-scale study of São Jorge Island, Azores archipelago', *Chemical Geology* **265**(3-4), 289–302.

Montanini, A. and Tribuzio, R. (2015), 'Evolution of recycled crust within the mantle: constraints from the garnet pyroxenites of the External Ligurian ophiolites (northern Apennines, Italy)', *Geology* **43**(10), 911–914.

Moreira, M., Doucelance, R., Kurz, M. D., Dupré, B. and Allègre, C. J. (1999), 'Helium and lead isotope geochemistry of the Azores Archipelago', *Earth and Planetary Science Letters* **169**(1-2), 189–205.

Moreira, M., Kanzari, A. and Madureira, P. (2012), 'Helium and neon isotopes in São Miguel island basalts, Azores Archipelago: New constraints on the "low 3He" hotspot origin', *Chemical Geology* **322**, 91–98.

Mukhopadhyay, S. (2012), 'Early differentiation and volatile accretion recorded in deep-mantle neon and xenon', *Nature* **486**(7401), 101–104.

Mundl, A., Touboul, M., Jackson, M. G., Day, J. M. D., Kurz, M. D., Lekic, V., Helz, R. T. and Walker, R. J. (2017), 'Tungsten-182 heterogeneity in modern ocean island basalts', *Science* **356**(6333), 66–69.

Mundl-Petermeier, A., Walker, R. J., Fischer, R. A., Lekic, V., Jackson, M. G. and Kurz, M. D. (2020), 'Anomalous 182W in high 3He/4He ocean island basalts: Fingerprints of Earth's core?', *Geochimica et Cosmochimica Acta* **271**, 194–211.

Mundl-Petermeier, A., Walker, R. J., Jackson, M. G., Blichert-Toft, J., Kurz, M. D. and Halldórsson, S. A. (2019), 'Temporal evolution of primordial tungsten-182 and 3He/4He signatures in the Iceland mantle plume', *Chemical Geology* **525**, 245–259.

Natland, J. H. (1980), 'The progression of volcanism in the Samoan linear volcanic chain', *American Journal of Science* **280**, 709–735.

Neave, D. A., Shorttle, O., Oeser, M., Weyer, S. and Kobayashi, K. (2018), 'Mantle-derived trace element variability in olivines and their melt inclusions', *Earth and Planetary Science Letters* **483**, 90–104.

Nebel, O., Sossi, P. A., Bénard, A., Arculus, R. J., Yaxley, G. M., Woodhead, J. D., Davies, D. R. and Ruttor, S. (2019), 'Reconciling petrological and isotopic mixing mechanisms in the Pitcairn mantle plume using stable Fe isotopes', *Earth and Planetary Science Letters* **521**, 60–67.

Nebel, O., Sossi, P. A., Benard, A., Wille, M., Vroon, P. Z. and Arculus, R. J. (2015), 'Redox-variability and controls in subduction zones from an iron-isotope perspective', *Earth and Planetary Science Letters* **432**, 142–151.

Nebel, O., Sossi, P. A., Foden, J., Bénard, A., Brandl, P. A., Stammeier, J. A., Lupton, J., Richter, M. and Arculus, R. J. (2018), 'Iron isotope variability in ocean floor lavas and mantle sources in the Lau back-arc basin', *Geochimica et Cosmochimica Acta* **241**, 150–163.

Palacz, Z. A. and Saunders, A. D. (1986), 'Coupled trace element and isotope enrichment in the Cook-Austral-Samoa islands, southwest Pacific', *Earth and Planetary Science Letters* **79**(3-4), 270–280.

Pertermann, M. and Hirschmann, M. M. (2003*a*), 'Anhydrous partial melting experiments on MORB-like eclogite: phase relations, phase compositions and mineral–melt partitioning of major elements at 2–3 GPa', *Journal of Petrology* **44**(12), 2173–2201.

Pertermann, M. and Hirschmann, M. M. (2003*b*), 'Partial melting experiments on a MORB-like pyroxenite between 2 and 3 GPa: Constraints on the presence of pyroxenite in basalt source regions from solidus location and melting rate', *Journal of Geophysical Research: Solid Earth* **108**(B2).

Peters, B. J., Carlson, R. W., Day, J. M. D. and Horan, M. F. (2018), 'Hadean silicate differentiation preserved by anomalous 142 Nd/144 Nd ratios in the Réunion hotspot source', *Nature* **555**(7694), 89–93.

Peters, B. J., Shahar, A., Carlson, R. W., Day, J. M. D. and Mock, T. D. (2019), 'A sulfide perspective on iron isotope fractionation during ocean island basalt petrogenesis', *Geochimica et Cosmochimica Acta* **245**, 59–78.

Plank, T. and Langmuir, C. H. (1998), 'The chemical composition of subducting sediment and its consequences for the crust and mantle', *Chemical geology* **145**(3-4), 325–394.

Polyakov, V. B. (2009), 'Equilibrium iron isotope fractionation at core-mantle boundary conditions', *Science* **323**(5916), 912–914.

Powell, R., Holland, T. J. B. and Worley, B. (1998), 'Calculating phase diagrams involving solid solutions via non-linear equations, with examples using THERMOCALC', *Journal of Metamorphic Geology* **16**(4), 577–588.

Prytulak, J. and Elliott, T. (2009), 'Determining melt productivity of mantle sources from 238U–230Th and 235U–231Pa disequilibria; an example from Pico Island, Azores', *Geochimica et Cosmochimica Acta* **73**(7), 2103–2122.

Putirka, K. (2008), 'Excess temperatures at ocean islands: Implications for mantle layering and convection', *Geology* **36**(4), 283–286.

Putirka, K. D. (2005), 'Mantle potential temperatures at Hawaii, Iceland, and the mid-ocean ridge system, as inferred from olivine phenocrysts: Evidence for thermally driven mantle plumes', *Geochemistry, Geophysics, Geosystems* **6**(5).

Putirka, K., Tao, Y., Hari, K. R., Perfit, M. R., Jackson, M. G. and Arevalo Jr, R. (2018), 'The mantle source of thermal plumes: Trace and minor elements in olivine and major oxides of primitive liquids (and why the olivine compositions don't matter)', *American Mineralogist: Journal of Earth and Planetary Materials* **103**(8), 1253–1270.

Qin, L. and Humayun, M. (2008), 'The Fe/Mn ratio in MORB and OIB determined by ICP-MS', *Geochimica et Cosmochimica Acta* **72**(6), 1660–1677.

Rapp, R. P., Irifune, T., Shimizu, N., Nishiyama, N., Norman, M. D. and Inoue, T. (2008), 'Subduction recycling of continental sediments and the origin of geochemically enriched reservoirs in the deep mantle', *Earth and Planetary Science Letters* **271**(1-4), 14–23.

Reinhard, A. A., Jackson, M. G., Blusztajn, J., Koppers, A. A. P., Simms, A. R. and Konter, J. G. (2019), '"Petit spot" rejuvenated volcanism superimposed on plume-derived Samoan shield volcanoes: Evidence from a 645-m drill core from Tutuila Island, American Samoa', *Geochemistry, Geophysics, Geosystems* **20**(3), 1485–1507.

Rizo, H., Andrault, D., Bennett, N. R., Humayun, M., Brandon, A., Vlastélic, I., Moine, B., Poirier, A., Bouhifd, M. A. and Murphy, D. T. (2019), '182w evidence for core-mantle interaction in the source of mantle plumes', *Geochemical Perspectives Letters* **11**, 6–11.

Rosenthal, A., Yaxley, G. M., Green, D. H., Hermann, J., Kovács, I. and Spandler, C. (2014), 'Continuous eclogite melting and variable refertilisation in upwelling heterogeneous mantle', *Scientific Reports* **4**, 6099 EP –.

Rouxel, O., Dobbek, N., Ludden, J. and Fouquet, Y. (2003), 'Iron isotope fractionation during oceanic crust alteration', *Chemical Geology* **202**(1-2), 155–182.

Rouxel, O., Fouquet, Y. and Ludden, J. N. (2004), 'Subsurface processes at the Lucky Strike hydrothermal field, Mid-Atlantic Ridge: evidence from sulfur, selenium, and iron isotopes', *Geochimica et Cosmochimica Acta* **68**(10), 2295–2311.

Salters, V. J. M. and Dick, H. J. B. (2002), 'Mineralogy of the mid-ocean-ridge basalt source from neodymium isotopic composition of abyssal peridotites', *Nature* **418**(6893), 68–72.

Schuessler, J. A., Schoenberg, R. and Sigmarsson, O. (2009), 'Iron and lithium isotope systematics of the Hekla volcano, Iceland—evidence for Fe isotope fractionation during magma differentiation', *Chemical Geology* **258**(1-2), 78–91.

Shahar, A., Schauble, E. A., Caracas, R., Gleason, A. E., Reagan, M. M., Xiao, Y., Shu, J. and Mao, W. (2016), 'Pressure-dependent isotopic composition of iron alloys', *Science* **352**(6285), 580–582.

Shorttle, O. and Maclennan, J. (2011), 'Compositional trends of Icelandic basalts: Implications for short–length scale lithological heterogeneity in mantle plumes', *Geochemistry, Geophysics, Geosystems* **12**(11).

Sobolev, A. V., Hofmann, A. W., Kuzmin, D. V., Yaxley, G. M., Arndt, N. T., Chung, S.-L., Danyushevsky, L. V., Elliott, T., Frey, F. A., Garcia, M. O. et al. (2007), 'The amount of recycled crust in sources of mantle-derived melts', *Science* **316**(5823), 412–417.

Sobolev, A. V., Hofmann, A. W., Sobolev, S. V. and Nikogosian, I. K. (2005), 'An olivine-free mantle source of Hawaiian shield basalts', *Nature* **434**(7033), 590–597.

Sossi, P. A., Nebel, O. and Foden, J. (2016), 'Iron isotope systematics in planetary reservoirs', *Earth and Planetary Science Letters* **452**, 295–308.

Sossi, P. A. and O'Neill, H. S. C. (2017), 'The effect of bonding environment on iron isotope fractionation between minerals at high temperature', *Geochimica et Cosmochimica Acta* **196**, 121–143.

Spice, H. E., Fitton, J. G. and Kirstein, L. A. (2016), 'Temperature fluctuation of the Iceland mantle plume through time', *Geochemistry, Geophysics, Geosystems* **17**(2), 243–254.

Stracke, A. (2012), 'Earth's heterogeneous mantle: A product of convection-driven interaction between crust and mantle', *Chemical Geology* **330**, 274–299.

Stracke, A., Hofmann, A. W. and Hart, S. R. (2005), 'FOZO, HIMU, and the rest of the mantle zoo', *Geochemistry, Geophysics, Geosystems* **6**(5).

Su, B.-X., Teng, F.-Z., Hu, Y., Shi, R.-D., Zhou, M.-F., Zhu, B., Liu, F., Gong, X.-H., Huang, Q.-S., Xiao, Y. et al. (2015), 'Iron and magnesium isotope fractionation in oceanic lithosphere and sub-arc mantle: Perspectives from ophiolites', *Earth and Planetary Science Letters* **430**, 523–532.

Sun, P., Niu, Y., Guo, P., Duan, M., Chen, S., Gong, H., Wang, X. and Xiao, Y. (2020), 'Large iron isotope variation in the eastern pacific mantle as a consequence of ancient low-degree melt metasomatism', *Geochimica et Cosmochimica Acta* **286**, 269–288.

Teng, F.-Z., Dauphas, N. and Helz, R. T. (2008), 'Iron Isotope Fractionation During Magmatic Differentiation in Kilauea Iki Lava Lake', *Science* **320**(5883), 1620–1622.

Teng, F.-Z., Dauphas, N., Huang, S. and Marty, B. (2013), 'Iron isotopic systematics of oceanic basalts', *Geochimica et Cosmochimica Acta* **107**, 12–26.

Turner, S., Hawkesworth, C., Rogers, N. and King, P. (1997), 'U-Th isotope disequilibria and ocean island basalt generation in the Azores', *Chemical Geology* **139**(1-4), 145–164.

Turner, S., Williams, H., Piazolo, S., Blichert-Toft, J., Gerdes, M., Adam, J., Liu, X.-M., Schaefer, B. and Maury, R. (2018), 'Sub-arc xenolith Fe-Li-Pb isotopes and textures tell tales of their journey through the mantle wedge and crust', *Geology* **46**(11), 947–950.

Urey, H. C. (1947), 'The thermodynamic properties of isotopic substances', *Journal of the Chemical Society (Resumed)* pp. 562–581.

Walker, R. J., Morgan, J. W. and Horan, M. F. (1995), 'Osmium-187 enrichment in some plumes: evidence for core-mantle interaction?', *Science* **269**(5225), 819–822.

Wang, C., Cascio, M. L., Liang, Y. and Xu, W. (2020), 'An experimental study of peridotite dissolution in eclogite-derived melts: Implications for styles of melt-rock interaction in lithospheric mantle beneath the North China Craton', *Geochimica et Cosmochimica Acta* **278**, 157–176.

Watanabe, S. (2010), Isotope and trace element investigation of magmatic processes and timescales in the Azores, PhD thesis, Miami University.

Waters, C. L., Day, J. M. D., Watanabe, S., Sayit, K., Zanon, V., Olson, K. M., Hanan, B. B. and Widom, E. (2020), 'Sulfide mantle source heterogeneity recorded in basaltic lavas from the azores', *Geochimica et Cosmochimica Acta* **268**, 422–445.

Weaver, B. L. (1991), 'The origin of ocean island basalt end-member compositions: trace element and isotopic constraints', *Earth and Planetary Science Letters* **104**(2-4), 381–397.

Weyer, S. and Ionov, D. A. (2007), 'Partial melting and melt percolation in the mantle: The message from Fe isotopes', *Earth and Planetary Science Letters* **259**(1-2), 119–133.

White, W. M. and Hofmann, A. W. (1982), 'Sr and Nd isotope geochemistry of oceanic basalts and mantle evolution', *Nature* **296**(5860), 821–825.

Williams, H. M. and Bizimis, M. (2014), 'Iron isotope tracing of mantle heterogeneity within the source regions of oceanic basalts', *Earth and Planetary Science Letters* **404**, 396–407.

Williams, H. M., McCammon, C. A., Peslier, A. H., Halliday, A. N., Teutsch, N., Levasseur, S. and Burg, J.-P. (2004), 'Iron Isotope Fractionation and the Oxygen Fugacity of the Mantle', *Science* **304**(5677), 1656–1659.

Williams, H. M., Nielsen, S. G., Renac, C., Griffin, W. L., O'Reilly, S. Y., McCammon, C. A., Pearson, N., Viljoen, F., Alt, J. C. and Halliday, A. N. (2009), 'Fractionation of oxygen and iron isotopes by partial melting processes: Implications for the interpretation of stable isotope signatures in mafic rocks', *Earth and Planetary Science Letters* **283**(1-4), 156–166.

Williams, H. M., Peslier, A. H., McCammon, C., Halliday, A. N., Levasseur, S., Teutsch, N. and Burg, J.-P. (2005), 'Systematic iron isotope variations in mantle rocks and minerals: the effects of partial melting and oxygen fugacity', *Earth and Planetary Science Letters* **235**(1-2), 435–452.

Williams, H. M., Prytulak, J., Woodhead, J. D., Kelley, K. A., Brounce, M. and Plank, T. (2018), 'Interplay of crystal fractionation, sulfide saturation and oxygen fugacity on the iron isotope composition of arc lavas: An example from the Marianas', *Geochimica et Cosmochimica Acta* **226**, 224 – 243.

Workman, R. K., Hart, S. R., Jackson, M., Regelous, M., Farley, K. A., Blusztajn, J., Kurz, M. and Staudigel, H. (2004), 'Recycled metasomatized lithosphere as the origin of the Enriched Mantle II (EM2) end-member: Evidence from the Samoan volcanic chain', *Geochemistry, Geophysics, Geosystems* **5**(4), n/a–n/a.

Wright, E. and White, W. M. (1987), 'The origin of Samoa: new evidence from Sr, Nd, and Pb isotopes', *Earth and Planetary Science Letters* **81**(2-3), 151–162.

Young, E. D., Manning, C. E., Schauble, E. A., Shahar, A., Macris, C. A., Lazar, C. and Jordan, M. (2015), 'High-temperature equilibrium isotope fractionation of non-traditional stable isotopes: Experiments, theory, and applications', *Chemical Geology* **395**, 176–195.

Yu, H. (2011), Li, Hf and Os isotope systematics of Azores basalts and a new microwave digestion method for Os isotopic analysis, PhD thesis, Miami University.

Zhao, X., Zhang, H., Zhu, X., Tang, S. and Yan, B. (2012), 'Iron isotope evidence for multistage melt–peridotite interactions in the lithospheric mantle of eastern China', *Chemical geology* **292**, 127–139.

Zindler, A. and Hart, S. (1986), 'Chemical geodynamics', *Annual review of earth and planetary sciences* **14**(1), 493–571.